UNIVERSITÀ
DI SIENA
1240

Department of Medical Biotechnology

Ph.D. in Genetic, Oncology and Clinical Medicine
(GenoMeC)
XXXV cycle

Inhibition of cyclin-dependent protein kinases as a potential new therapeutic strategy for the treatment of malignant pleural mesothelioma

Doctorate Cordinatore:
Prof. Francesca Ariani

Candidate:
Aurora Costa

Tutor:
Prof. Antonio Giordano

Matr:
094672

Supervisor:
Dr. Mario Chiariello

Siena, March 21st, 2023

Table of Contents

ABSTRACT

Direct or indirect exposure to asbestos fibers can cause various respiratory pathologies such as asbestosis or pleural effusion, up to more serious pathologies, even tumors such as malignant pleural mesothelioma (MPM).

MPM is a highly aggressive tumor for which there is still no effective therapeutic strategy today and, despite the use of asbestos being banned in many western countries, unfortunately an increase in incidence is still estimated. This is due both to the long clinical latency that characterizes the development of MPM (about 40 years), and to the environmental persistence of materials containing asbestos. To date, MPM still represents a therapeutic challenge, and therefore, the identification of new and effective therapies is urgently needed.

In recent years various approaches have been tested in the preclinical phase by the group where I carried out my thesis activity, such as the inhibition of the oncogenic kinase SRC, or the reactivation of p53, both capable of inducing cell death both in MPM lines than in *in vivo* experiments. More recently they observed that reactivation of the RBL2/p130 tumor suppressor was also able to induce apoptosis in MPM cell lines. These data suggested that acting by restoring the function of retinoblastoma family proteins could be an effective strategy for this tumor.

The aim of my thesis project was to verify whether the inhibition of the cyclin-cycline kinase dependent complexes, more specifically using the cyclin dependent kinase (CDK) inhibitor abemaciclib, was able to act on the pocket proteins, reactivating their tumor suppressor potential.

First of all, we demonstrated that abemaciclib dose-dependently inhibits the cell proliferation in short- and long-term of MPM cell lines, however, it did not show the same cytotoxic effects on the mesothelium cell line used as a control. Subsequently, we tested and confirmed that abemaciclib is able to induce apoptosis in some MPM lines by cytofluorimetric assay of annexin. In Addition, we then evaluated the ability of abemaciclib on 3D cell cultures, drug showed the capacity inhibiting the formation of 1st and 2nd generation spheroids but also blocking the proliferation of fully formed spheroids. Again, to investigate the molecular mechanism through which the inhibitor acts, by western blotting, the phosphorylation levels of all three pocket proteins (RBL2/p130, RBL1/p107 and RB1/p105) were evaluated, as expected. The inhibitor induces a reduction in p130 (Ser952) and (Ser941), p107 (Ser975), and p105 (Ser780) phosphorylation with consequent restoration of protein functionality.

Moreover, since previous studies demonstrate that reactivation of the RBL2/p130 tumor suppressor mediates apoptosis in MPM cell lines by counteracting the AKT-activated antiapoptotic pathway, we tested the levels of AKT protein and its phosphorylation, and how we expected this drug induces reduction of AKT phosphorylation (Ser473).

Finally, we decided to evaluate the sensitivity to abemacilib on ciplatin-resistant cells, and the results show that the more aggressive mesotlioma cells remained sensitive to this drug even though resistant to cisplatin. The data obtained are certainly still preliminary, the subsequent studies are necessary above all to understand what happens to the progression of the cell cycle, but at the same time, they are promising, urging us to continue and making us hypothesize that this treatment could be effective for patients with MPM.

1. INTRODUTION

1.1 Mesothelium

The mesothelium is a monolayer of specialized cells, mesothelial cells, surrounding the entire surface of serosal cavities such as:

- pleural,
- pericardial,
- peritoneal,
- in males, it also lines the sac around the testes.

Mesothelial cells lay on a thin basement membrane supported by connective tissue stroma, with the stroma, which differ in amount and quality according to the area and species[1].

The major role of the mesothelium is to create a frictionless, free surface, which allows encourages movement across the pleural, pericardial, and peritoneal cavities. This is accomplished through the mesothelium's ability to act as a free surface, using a limited amount of viscous fluid in conjunction with a unique adaptation of the luminal surface of the cell [2].

In addition to acting as a protective, non-adhesive surface, the mesothelium is involved in the movement of solutes and cells through serosal cavities, the presentation of antigens, inflammation and tissue healing, coagulation and fibrinolysis, and the adherence of tumour cells[1]

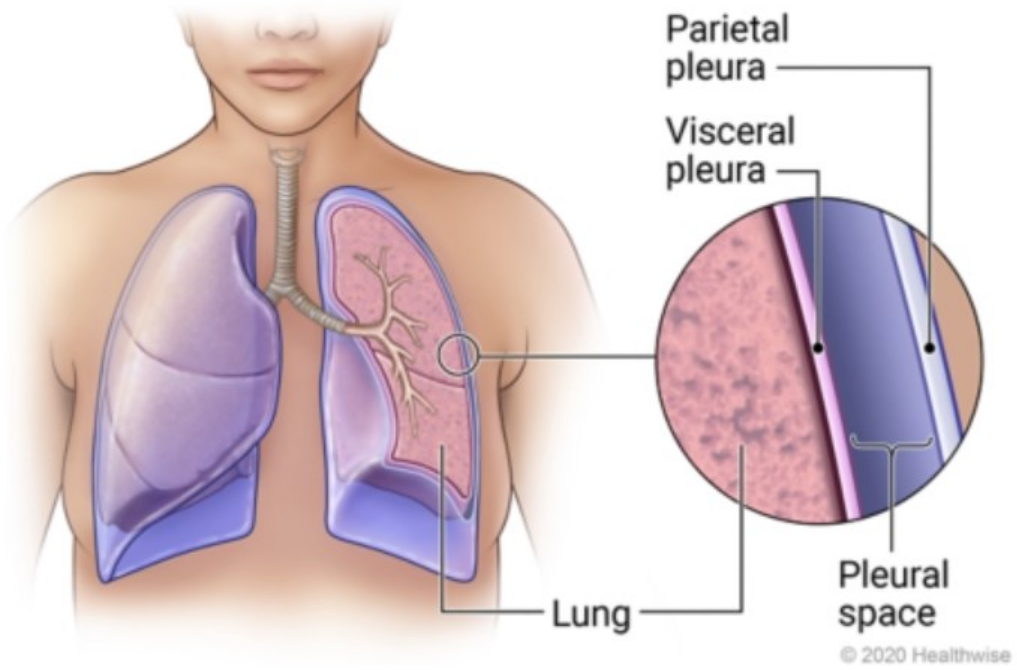

Figure 1. Structure of pleura (Healthwise Staff, 2021)

The pleura consists of two thin layers of tissue, which protect and cushion the lungs. The inner layer (visceral pleura) wraps around the lungs and is very firm and protective around the lungs. The outer layer (parietal pleura) borders the internal chest wall. The region between the layers is known as the pleural space, which contains pleural fluid. The fluid lubricates the pleural space, allowing the two layers of pleural tissue to slide against one another.

Furthermore, pleural mesothelial cells are necessary for maintaining the proper homeostasis of the pleural space and are key components of pathophysiologic events influencing the pleural space[3].

1.2. Malignant Mesothelioma

Malignant mesothelioma (MM) is a very aggressive tumour with a poor prognosis, it is difficult to diagnose and arises from mesothelial cells covering the serous membranes around numerous organs and tissues. The disease is strongly linked to asbestos exposure with an etiological fraction of 80% or more[4], with a latency period of ~40 years between fiber exposure and disease presentation[5].

There are two types of mesothelium tumours. Benign forms, which are localized, slow-growing tumours that are often surgically eradicated and do not need further treatment, and the incidence has grown dramatically over the last 30 years[5].

MM mainly affects the pleura (93.9%), as well as the peritoneum (5.8%), tunica vaginalis (0.3%), and pericardium (0.1%) [6].

Malignant Pleural Mesothelioma (MPM) is the most common mesothelioma type [7]. It infiltrates the pleura extensively, resulting in pleural effusion and substantial impairment of respiratory function. The most recent categorization of the World Health Organization (WHO) divides MPM into three major categories[7] [8]:

- epithelioid, (50–70% of cases)
- sarcomatoid, (10–20% of cases)
- biphasic (30% of cases)

Epithelioid mesothelioma (EM) is characterized by oval, cuboidal or spindle-shaped epithelioid cells that infiltrate the pleura in a tubular or papillary developmental pattern. However, a variety of architectural growth patterns may be observed, such as trabecular, solid, micropapillary, and, less frequently, adenomatoid and microcystic.

According to the WHO classification [8], the second most frequent form of mesothelioma is **Sarcomatoid mesothelioma**, which is a proliferation of spindle cells that penetrate adipose tissue or lung parenchyma and are organized in fascicles or random patterns.

Biphasic mesotheliomas are constituted of both epithelioid and sarcomatoid morphology, and at least 10% of each component is necessary in resection specimens for a definite diagnosis. Histological subtypes continue to be the most important factor in determining a patient's prognosis for mesothelioma [9]. Sarcomatoid mesothelioma has the worst prognosis, with a median survival of 4 months, compared to 8.4 months, biphasic mesotheliomas while the epithelioid histology confers the most favorable prognosis of 13.1 months [10] [11] [12] [13]. **(Fig. 2)**

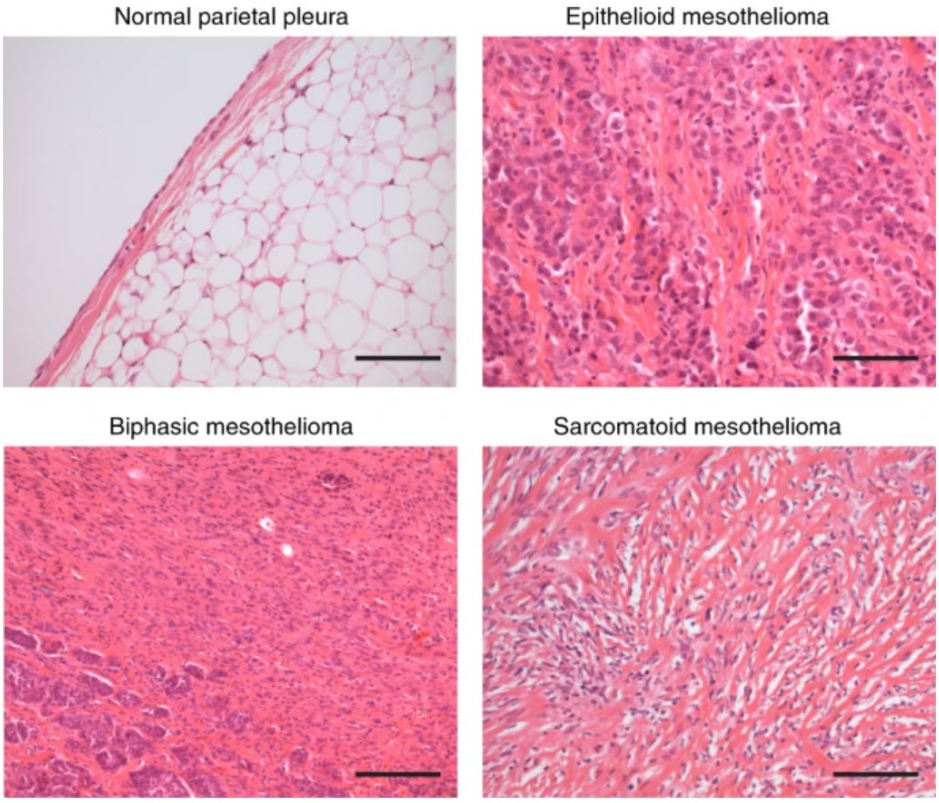

Figure 2 Histopathological classification of malignant mesothelioma. Images of haematoxylin and eosin (H&E) stained normal pleura (×100), epithelioid (×100), sarcomatoid (×100) and biphasic (×100) mesothelioma subtypes, indicating the presence of flat, cuboidal cells in epithelioid mesothelioma as well as spindle cells and abundant stroma in sarcomatoid mesothelioma. Scale bar = 200 μm. The images were provided by Royal Papworth Hospital Research Tissue Bank [14].

1.3 Etiopathogenesis

MPM is one of cancers for which there is strong etiopathogenetic certainty as in fact, this disease is linked to asbestos exposure with an etiological fraction of 80% or more. In addition to exposure to this mineral, other risk factors include erionite (a mineral found in the rocks of Turkey), ionizing radiation, long straight carbon nanotubes, genetic predisposition, and the Simian virus 40. (SV40). The latter, an oncogenic virus that inhibits tumour suppressor genes, could operate as a cofactor in the development of MPM, but proof of causation is limited. Asbestos and SV40 are now believed to serve as co-carcinogens, but its involvement has long been the subject of controversy [15].

Would a single amphibole asbestos fiber enhance the risk of lung cancer or mesothelioma? Traditional linear no-threshold (LNT) risk assessment assumptions suggest that the response is affirmative: there is no safe exposure level [16].

Asbestos is a naturally occurring mineral with a microcrystalline structure and a fibrous appearance. It belongs to the chemical class of silicates and can have two distinct structural forms: the curly and serpentine fibers of chrysotile or "white" asbestos and the sharp and needle-like amphibole asbestos [17]. Asbestos is an umbrella word representing six silicate minerals that can form very thin fibers, the serpentine group (chrysotile) and the amphibole group of minerals (crocidolite, amosite, anthophyllite, tremolite and actinolite). Chrysotile is less bio-persistent in the lungs than amphiboles. Chrysotile, amosite, and crocidolite have all been widely used for industrial purposes.

To date, a dose–response relationship between asbestos exposure and the occurrence of mesothelioma has been defined [13].

Exposure to asbestos fibers can be [14]:

• **Direct**, due to occupations where asbestos was used.

• **Indirect**, as a result of family members of employees who used asbestos (work clothes).

Indeed, incidence and mortality rates varied in regions where asbestos was used industrially, such as naval shipyards, asbestos–cement facilities, and others [18]. Although asbestos utilization has been prohibited in many countries, some variants are still mined and used globally. In addition, other mineral fibers comparable to asbestos are not even controlled [18]. Thus, therefore there is serious concern for the future emergence of more MPM cases [19].

Additionally, the perceived danger linked with environmental exposure has climbed [20]. A further cause for alarm is that the latency period for MPM is often three or four decades following the first

asbestos exposure; as a consequence, a considerable number of cases are still predicted in numerous countries [21]. In the case of asbestos inhaled microscopic fibers relocate to the pleural region, where they might remain for decades, triggering mitogenic and inflammatory pathways. Local production of reactive oxygen species by asbestos fibers seems to culminate in DNA damage, therefore initiating malignant transformation [14].

Some studies have demonstrated the critical role of TNF-α and NF-kB in the response of mesothelial cells to asbestos exposure. Following exposure to asbestos, an inflammatory reaction is evoked, macrophages uptake asbestos fibers and release TNF-α [22]. At the same time, asbestos induces the expression of the TNF-α receptor TNF-R1 in primary human mesothelial cells (HM), which in turn release TNF-α. Thus, a paracrine and autocrine mechanism is generated by asbestos [22].

TNF-α, upon binding to the receptor on mesothelial cells, activates NF-κB, which leads to survival of HM. Consequently, the surviving mesothelial cells accumulate DNA damage [23].

In addition, because of asbestos toxicity, there is an increase of free radicals (reactive oxygen and nitrogen species generated by further damage to the cellular genetic material. TNF-α signaling, through NF-κB-dependent mechanisms, increases the percentage of HMs surviving asbestos exposure, thereby increasing the pool of asbestos-damaged HMs susceptible to malignant transformation [23]. **(Fig.3)**

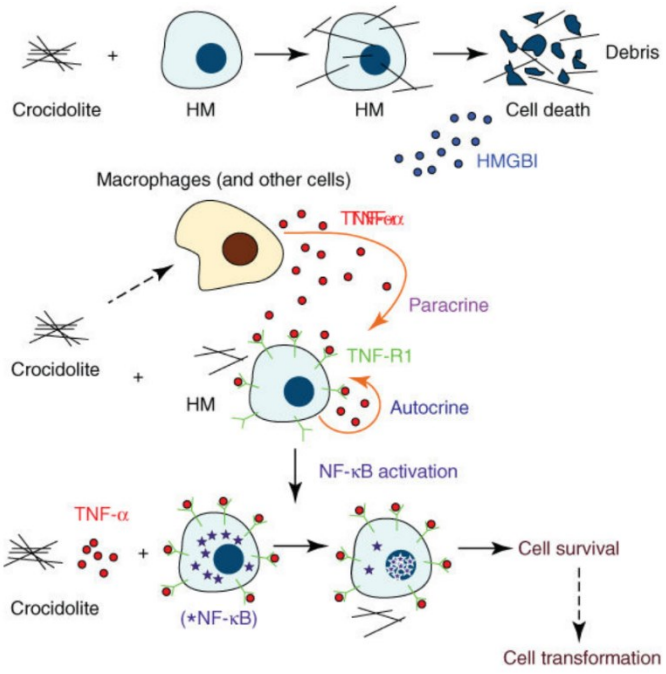

Figure 3 Schematization of one of the potential oncogenesis mechanisms exerted by the inhalation of asbestos fibers.

As said, asbestos fibers penetrate mesothelial cells and interfere with mitosis, generate mutations in DNA and change chromosomal structure. Mesothelial cells exposed to asbestos release inflammatory cytokines, including tumor growth factor-β, and growth factors such as platelet-derived growth factor, and vascular endothelial growth factor (VEGF). This creates a favorable microenvironment for tumor growth [15].

Finally, asbestos induces phosphorylation of various protein kinases leading to increased expression of proto-oncogenes and further promotion of abnormal cell proliferation [15].

Recently published data have demonstrated a genetic component associated with increased risk of mesothelioma in subjects with mesothelioma-diagnosed parents or siblings, namely a germline mutation of the BRCA1-associated protein 1 (*BAP-1*) gene, a tumour suppressor gene involved in the regulation of transcription and DNA repair. Other genes, which might affect predisposition to MPM are cyclin-dependent kinase inhibitor 2A (CDKN2A), NF2, LATS2, and TP53 [24].

1.4 Epidemiology

The incidence of MPM peaks in the fifth and sixth decades of life and is more prevalent in males than women[25].

About to 10% of all cases are diagnosed in patients younger than 55 years old. 34.2% of patients are between the ages of 65 and 74. The proportion of males vs females affected by the malignancy varies by country. In North America, this ratio is approximately 9:1. However in other nations, as England, France, Australia, or Italy, it is 2-3:1[26].

MPM is the subject of a particular epidemiological survey conducted by the National Mesothelioma Register (ReNaM), which was formed in accordance with Legislative Decree 257/1992, which prohibited the use of asbestos in Italy.

In Italy, the ReNaM documented 21,463 cases of MM between 1993 and 2012, approximately 1,073 occurrences per year. 93% of these cases were pleural mesothelioma. For 77% of MM cases, the routes of asbestos exposure were identified and 10.5% were non-occupational (including 4.2% environmental) while 69.5% were occupational exposures [26].

The VI Report of the ReNaM, released in November 2018 and presenting data up to 2015, showed an average of 1,594 incident instances of mesothelioma each year between 2013 and 2015, with 1,496 occurrences occurring in the pleural site.

1.5 Symptoms

MPM presents with nonspecific symptoms, such as shortness of breath, pain in the chest, dyspnea, and weight loss. On chest imaging, pleural anomalies that include a unilateral effusion, calcified plaques, thickness, or masses are characteristic [27].

At presentation, 70% of patients have a pleural effusion, which causes breathlessness. As the disease advances, pleural effusions decrease due to medicinal intervention or tumour obliteration [28]. Breathlessness results from the tumour encasing the lung and restricting respiratory movement across the pleural surface.

Effusions and tumours can cause chest pain. It feels dull, heavy, and "dragging". In parietal pleural irritation, pleuritic discomfort is rare. If the illness invades the chest wall, chest pain worsens. Rib invasion or intercostal nerve involvement can also cause bone discomfort [29].

MPM also causes fatigue, anorexia, weight loss, sweating, and malaise [28]. Both tumour and host cytokines cause this. MPM has less cough, haemoptysis, and lymphadenopathy than bronchogenic tumours. Local tumour invasion might produce superior vena cava blockage, laryngeal nerve palsy, or dysphagia [29].

Some asymptomatic patients have imaging abnormalities. Asymptomatic patients may survive longer due to earlier diagnosis. Even if the pleural effusion is minor or resolves spontaneously, patients with a history of asbestos exposure should be closely monitored. Active follow-up improves the likelihood of early MPM diagnosis in these patients [15].

1.6 Diagnosis

MPM is a difficult disease to diagnose. All patients should have radiological imaging because it provides essential diagnostic and staging information.

A full-thickness pleural biopsy via pleuroscopy or video-assisted thoracoscopy is frequently required for diagnosis. Even though pleural fluid cytology is simpler to obtain, it is typically insufficient. Although with appropriate tissue, pathologic examination can be difficult considering

mesothelioma is uncommon in most facilities and there are numerous subtypes that must be distinguished from reactive pleural diseases [30].

MPM is hard to diagnose and among the investigations that can be performed we have radiological imaging which can provide valuable diagnostic and staging information. However, radiological interpretation can be difficult if pleural thickening is minimal or absent, and staging is often difficult due to the heterogeneous growth pattern of the tumor [15].

Chest X-ray is usually the first investigation done. However, chest radiographs are usually insensitive and nonspecific, and additional imaging is usually required [15]. **(Fig. 4)**

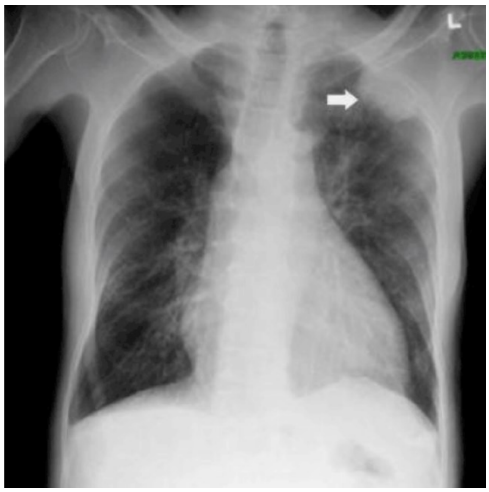

Figure 4 Radiography of the patient revealing pleural-based opacity left upper lung field. Also cardiomegaly and mild pulmonary congestion may be noted [31].

Thoracic ultrasound of the patient is commonly done to evaluate the volume, distribution, and echogenicity of the pleural fluid and to determine a safe site for aspiration. However, the sensitivity is low than the 40% require further investigation if MPM is suspected [15].

CT imaging is important in patients with MPM. Some studies have reported high sensitivity and specificity associated with these characteristics; however, appearances can be subjective and are highly operator dependent [15].

Further imaging can be done with positron emission technology (PET-CT) or magnetic resonance imaging (MRI) [15].

Biomarkers are useful diagnostic and prognostic tools, but they have limited clinical use for MPM. **Mesothelin** is a cell adhesion glycoprotein expressed in normal mesothelial cells of the pleura, but highly expressed in MPM. The utility of mesothelin has been demonstrated in clinical applications such as the differential diagnosis between malignant pleural mesothelioma and respiratory diseases, monitoring of response to MPM therapeutic treatment, as well as independent prognostic factor. Other biomarkers that have been explored in MPM include **megakaryocyte enhancer factor** (an alternative cleavage product of mesothelin precursor protein), **osteopontin and fibulin 3 glycoprotein**s. Osteopontin (OP) is a multifunctional glycoprotein secreted into all body fluids, present in the bone, but also in various cell types including macrophages, endothelial cells, epithelial cells. It is overexpressed in various tumours, including MPM, and correlates with tumor invasiveness, progression and metastasis [32].

A suspected MPM requires sampling of pleural fluid for biochemical and cytological examination. Unfortunately, cytological yield is low in MPM and biopsies are usually required to confirm the diagnosis and identify histological subtypes [29].

1.7 Therapeutic strategies

A multimodal approach is generally preferred to increase treatment efficacy and achieve optimal survival rate. The latter can be applied in both curative and palliative settings [25][33].

The management of mesothelioma is a multimodal strategy incorporating chemotherapy, surgery, and/or radiation [34]. However, the prognosis of MPM has not significantly improved over the past 20 years, with a 5-year survival of 7% [25].

The initial step is evaluating whether the disease is surgically respectable, with the goal of macroscopically complete resection. Surgery is the most common treatment with curative or palliative purpose, and according to the latest guidelines it is mainly indicated in multimodal approaches. Curative surgery is aimed at total removal of the tumor, which must be optimally localized, while in the case of palliative surgery, when the tumor has already spread, is aimed at reducing symptoms.

There are two main surgical techniques are with radical and curative intent:

1. extra pleural pneumonectomy (EPP)
2. the less radical pleurectomy/ decortication (P/D). [35]

A recent meta-analysis revealed that P/D had a lower short-term mortality rate than EPP, but that the 2-year survival rate does not differ significantly. The surgical strategy is selected patient-by-patient in the absence of randomised trial data.[35]

For a long time, EPP was the most used approach because it was considered the only way to obtain a complete macroscopic resection. In recent years, extended P/D has been preferred over EPP because it has shown significantly lower complication rates, lower perioperative morbidity, and mortality, and similar overall survival rates [35].

Chemotherapy could be a single drug or a combination of drugs to destroy cancer cells. If chemotherapy is performed before surgery, it is called **neoadjuvant chemotherapy**, while if the drug is administered after the operation, it is called **adjuvant chemotherapy**.

Chemotherapy is recommended for all patients getting active treatment for MPM, with cisplatin or carboplatin combined with pemetrexed as standard of care. In patients unsuitable for surgical resection, cisplatin/pemetrexed demonstrated higher median overall survival of 12.1 versus 9.3 months compared to cisplatin monotherapy [36].

Carboplatin is as effective as cisplatin when used with pemetrexed, making it a viable option for elderly patients and those with impaired renal function [36]. The addition of bevacizumab to cisplatin/pemetrexed could provide additional benefits, increasing the median overall survival to 18 months [37]. Pemetrexed and raltitrexed are folate antimetabolites that function by interfering with nucleic acid synthesis [38]. Chemotherapy is administered preoperatively or postoperatively to patients undergoing surgical resection, with no data comparing the two procedures.

Most studies have evaluated **radiation therapy** in post-surgery setting to lower the risk of local recurrence [39]. **Trimodal therapy** including pre-surgery chemotherapy, surgical resection, and post-surgery radiation has been tested in limited studies with varying degrees of success [40] [41].

Intensity Modulated Radiation Therapy (IMRT) is a sophisticated modality that uses small beams of radiation at various angles in a 3-dimensional conformal pattern, allowing for more intense radiation to hit the target with greater accuracy [42]. The application of IMRT can be preoperative (SMART) and postoperative (IMPRINT).

Radiation therapy can also be used as part of a trimodal approach. IMRT after chemotherapy and lung-sparing pleurectomy has been shown to be a safe approach [42]

Finally, in the field of **immunotherapy** there are encouraging data for the treatment of MPM. Specifically, programmed cell death 1 (PD-1) inhibitors (e.g., pembrolizumab, nivolumab) or programmed cell death 1 (PD-L1) ligand inhibitors (e.g., avelumab) showed response rates of 9-28 % and disease control rates of 57–76%. However, in these studies, survival is relatively short[43].

The majority of MPM patients are only eligible for palliative treatment and have a median overall survival of 1–2 years in spite of administration of multimodality therapy [43]. These limitations of

present treatment emphasize the need for innovative therapeutics, which could improve the prognosis of this fatal disease.

1.8 Drug Resistance

Drug resistance is the major obstacle to cancer therapies. The problem of resistance to therapy in cancer is multifaceted problem.

Intrinsic and extrinsic aggressors proliferate rapidly and represent an obstacle to the problem of drug resistance in cancer. The initial success of early chemotherapeutics (such as nitrogen mustard [44] and aminopterin [45]) was quickly tempered by evidence demonstrating that, although tumours went into remission fast, they developed resistance, resulting in disease relapse [46]. The first approach used to overcome single-agent chemotherapy resistance was polychemotherapy [47]. In breast, testicular, and lymphoma, this technique performed well [48]. Thus, combination chemotherapy led to more sophisticated cancer treatments. In addition, shorter-interval chemotherapy or higher-dose chemotherapy [49] with growth factor support to minimize bone marrow suppression benefited these regimens by inhibiting early tumour regrowth [46].

Cisplatin and carboplatin, along with antimetabolites like pemetrexed or gemcitabine, are approved for mesothelioma treatment [50]. Cisplatin is limited by significant side effects and medication resistance. 50% of cisplatin-treated individuals develop intrinsic or fast multidrug resistance. Cisplatin penetrates cells via many mechanisms, produces several DNA-platinum adducts, and activates or silences a range of genes, causing significant epigenetic and genetic changes. Thus, cisplatin resistance in human cancer cells *in vivo* and *in vitro* requires complicated genetic and epigenetic gene expression and protein localization modifications [50]. Apoptosis, developmental processes, DNA damage repair, endocytosis, and cell growth pathways all change.

Cisplatin-resistant cells affect dozens of genes, including copper metabolism pathways and transcription pathways that modify the cytoskeleton, cell surface protein presentation, and epithelial-to-mesenchymal transition. Cisplatin resistance often results from decreased accumulation [50].

Increasing expression levels of several transporters and increased repair of platinum-DNA adducts are regarded as the two most important steps in the development of drug resistance. Platinum drug response prediction is increasingly dependent on functional genomics [51].

1.9 Cell Cycle

To divide and multiply, all eukaryotic cells must comply a correct cell cycle, which allows a proper replication and segregation of hereditary material into daughter cells [52].

The cell cycle is a complex process and involves several regulatory proteins and consists of an ordered sequence of phases:

• **G1 phase**, also known as the first-gap phase. In this phase, cells grow in size, synthesize cell organelles and other macromolecules such as proteins. The cells also accumulate sufficient energy required for division [52].

• **S phase,** also known as the synthesis phase. DNA is copied within the nucleus. This process of DNA synthesis is also known as DNA-replication. The centrosome is also duplicated during this phase and gives rise to spindle fibers. The entire S-phase requires energy expenditure to proceed [52].

• **G2 phase**, this is the second gap phase and is somewhat similar to the G1-phase. During this period, the cells grow further in size, making more proteins and organelles. All preparations for mitosis get completed before the cells enter the mitotic phase [52].

• **M phase**, or **mitosis**, it is the nuclear division period and consists of four phases: prophase, metaphase, anaphase, and telophase. During this phases, cells divide the nucleus and gets separated into two daughter cells, where each daughter cell receives a complete set of chromosomes [52].

(Fig. 5)

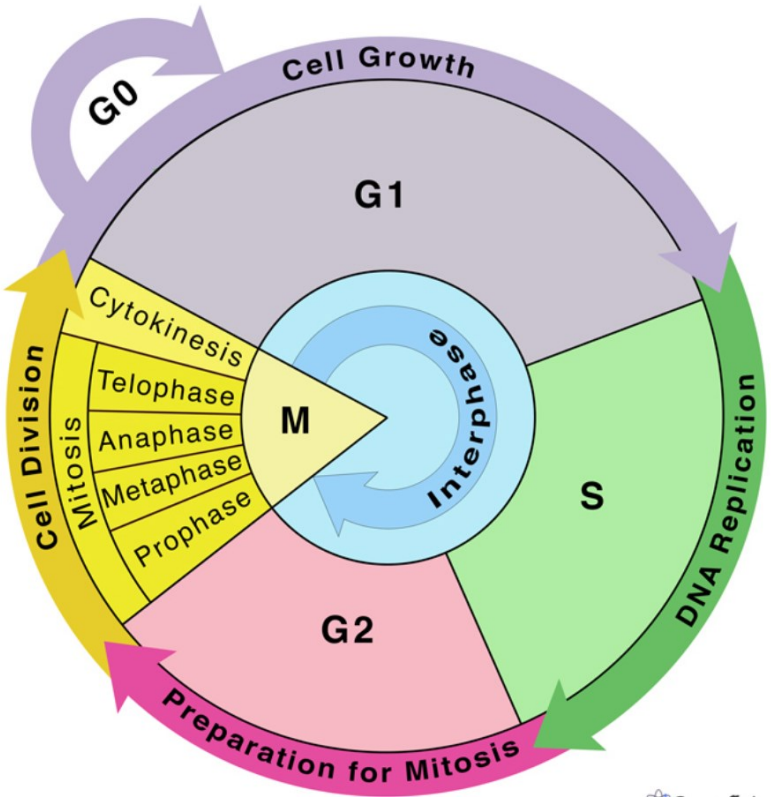

Figure 5 Cell Cycle diagram of sequence of phases: G1 phase, during which the cell prepares for DNA synthesis; S phase, during which DNA is replicated; G2 phase, during which the cell prepares for mitosis; M phase or mitosis, during which cells segregate into daughter cells.

The cell cycle is a highly regulated process. There are “checkpoints” for managing the system and determine whether cells will start or postpone the next phase of the cell cycle [52].

Numerous regulatory proteins lead the cell through a specified sequence of events, culminating in mitosis and the formation of two daughter cells. Cyclin-dependent kinases (CDKs), which form a complex with cyclin proteins, are essential in the cell cycle process. These proteins regulate the passage of the cell through the stages of the cell cycle and are themselves regulated by other proteins, including p53, p21, p16, and cdc25. pRb and E2F are targets downstream of cyclin-CDK complexes. In neoplasia, the cell cycle is frequently dysregulated because to mutations in oncogenes that indirectly effect the cell cycle or in tumor suppressor genes or oncogenes that directly impact cell cycle regulation, such as pRb, p53, p16, Cyclin D1, or mdm-2 [53].

1.10 Retinoblastoma Proteins

The retinoblastoma (Rb) family includes three members: RBL2/p130, RBL1/p107 and, RB1/p105 collectively referred to as ‘pocket proteins’ [54]. Those proteins are tumor suppressor gene first identified in a malignant tumor of the retina known as retinoblastoma [54].

Pocket proteins have extensive similarity, particularly in the bipartite region known as the 'pocket domain'. RBL2/p130 and RBL1/p107 have 50% amino acid identity and are more closely related than RB1/p105 (30–35% identity). Retinoblastoma family proteins have a distinctive steric shape due to the pocket region, which is responsible for many of the protein–protein interactions in cell cycle homeostasis. The pocket domain is characterized structurally by two conserved functional domains (A and B) separated by a spacer (S) that vary significantly among the three proteins, RB1/p105, RBL2/p130, and RBL1/p107. Members of the E2F family of transcription factors are cellular Rb-binding proteins and interact with the A and B pocket domains [54].

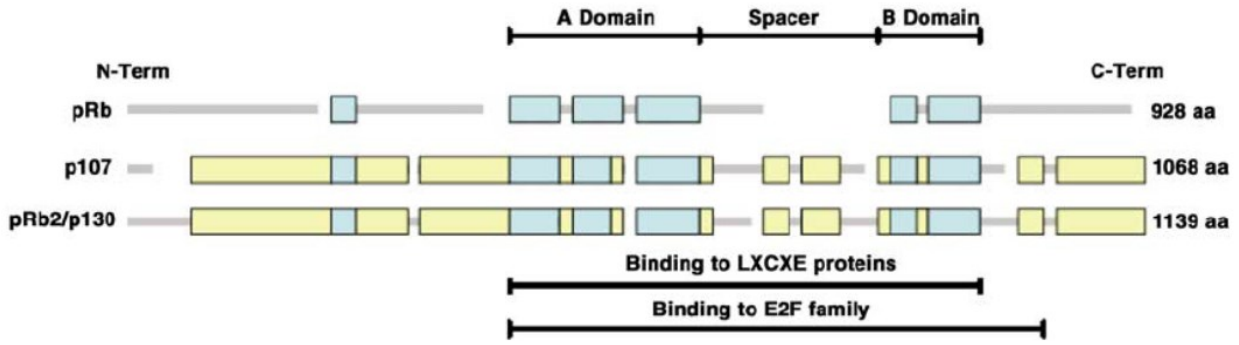

Figure 6 Proteins pockets structure [55]

The Rb proteins are a tumour suppressor and plays a crucial part in the negative regulation of the cell cycle and the growth of tumoursand cancer growth. They are important keys forG1 checkpoints, inhibiting S-phase entry and cell proliferation and they inhibit gene transcription, which is necessary for the transition from G1 to S phase, by directly binding to the transactivation domain of E2F and the promoter of these genes in complex with E2F. Pocket proteins phosphorylation mediated by cyclin-CDK complexes limits their binding capacity to targets, thereby negatively regulating RBL2/p130, RBL1/p107 and RB1/p105's action as tumor suppressor. For instance, phosphorylation events modulated initially by the cyclin D-CDK 4/6 complex and subsequently by cyclin E-CDK2 inactivate RBL2/P130, RBL1/P107 or RB1/p105 as in fact CDK4/CDK6, along with CDK2, are the principal kinases responsible for phosphorylating pocket proteins. Through the control of E2F-responsive genes, these proteins inhibit the G1–S transition. In addition to influencing the G1–S transition via E2F-independent pathways, such as via suppressing CDK2 or stabilizing p27 ^{Kip1}, pocket proteins are also involved in the regulation of G0 exit, the spatial organization of replication, and genomic replication [56].

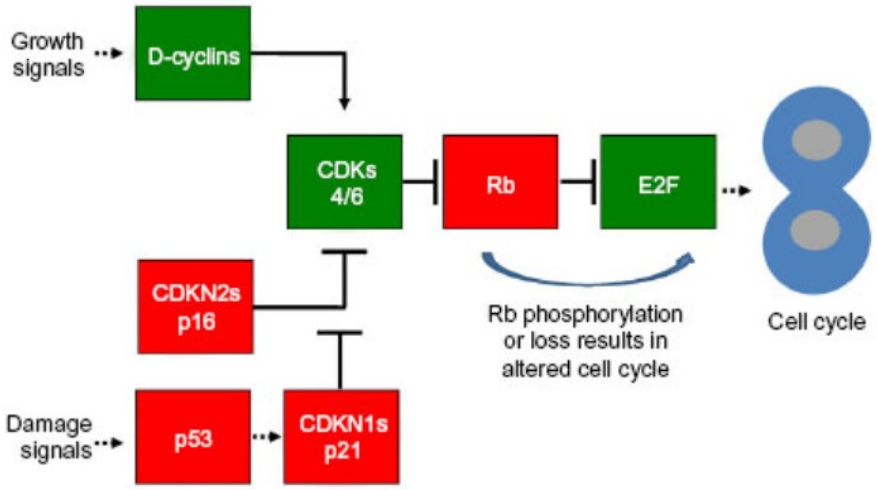

Figure7 This diagram illustrates the canonical CDK/Rb/E2F pathway. In this model, tumor suppressor proteins are indicated in red ("stop" light), whereas proteins promoting tumor growth are highlighted in green ("go" light). Solid pointed arrows denote a direct activation event, such as cyclins binding CDKs. Solid blunt arrows denote direct inactivation through direct binding (such as Rb binding E2F to block its transcriptional activity) or by protein modification (such as the phosphorylation of Rb by CDKs, which renders it incapable of binding and repressing E2F). Lines with dashes represent indirect regulation [57].

After the S, G2, and M phases of the cell cycle, pocket proteins are dephosphorylated and bind to transcription factors, sequestering them until the succeeding cell cycle [54].

During the transition between the G0/G1/S phases of the cell cycle, expression levels of RB family members change. RB1/p105 is constitutively expressed during all phases of the cell cycle, whereas RBL1/p107 is mostly expressed during the S phase while RBL2/p130 expression peaks during the G0 phase [58] **(Fig.8)**.

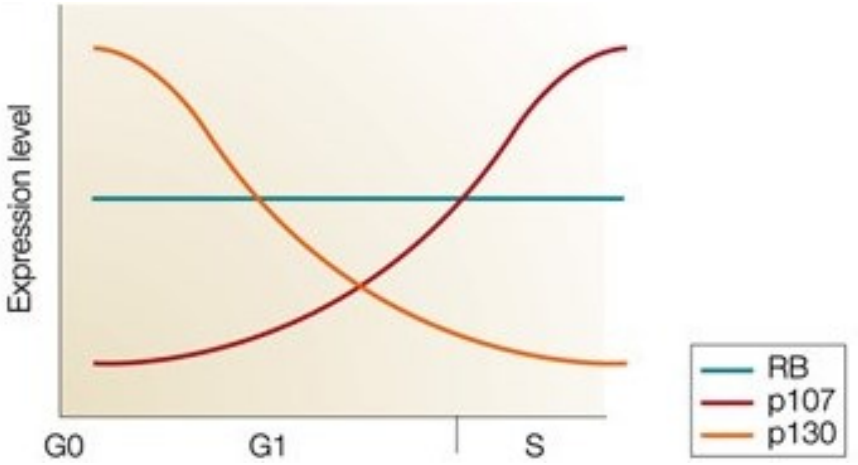

Figure 8 Expression levels of retinoblastoma family proteins during cell cycle progression.

Because of the frequent dysregulation of RB proteins and their pathways in cancer, numerous attempts are currently underway to using therapies based on their reactivation [59]. Specific approaches have been developed for restoring the cell cycle by inhibiting CDK and restore the role of RB [59].

1.11 Cell cycle regulators

The cell cycle process is governed by numerous proteins with key functions. Among these, Cyclin-Dependent Kinase Inhibitors (CKIs), suppress cell proliferation. CKIs bind cyclin-CDK dimers, thereby inhibiting them and negatively regulating cell proliferation [60].

CKIs can be divided into two groups:

- The first class, called "**inhibitor of CDK**" or INK4, includes the proteins **$p16^{INK4a}$, $p15^{INK4b}$, $p18^{INK4c}$ and $p19^{INK4d}$** which are specific for CDK 4 and CDK 6 and inhibit binding to cyclin D [61]. Overexpression of INK4 proteins causes G1-phase cell cycle arrest in a RB-dependent manner, as hypophosphorylated RB binds and inactivates E2F, promoting cell cycle arrest [60];
- The second class, the **Cip/Kip** family, includes the proteins **$p21^{Cip1/WAF1}$, $p27^{Kip1}$ and $p57^{Kip2}$** which are general inhibitors of Cdks, but are capable of specifically blocking the kinase activity of Cdk4 and Cdk2 [61]. Proteins of the Cip/Kip family exclusively bind and inhibit cyclin-CDK complexes that act during G1 and S phases [60].

Definitely, Cip/Kip and INK4 proteins are essential regulators of cell proliferation. Defect in these proteins causes dysregulation of cell cycle, apoptosis and DNA repair mechanisms.

Consequently, approaches aimed at restoring or mimicking their function could be exploited as therapies against different forms of neoplasms.

Retinoblastoma family proteins are substrates of the CDK complexes CDKs phosphorylate Rb family proteins in order to promote the release of transcription factors (E2F), thereby allowing the expression/repression of genes specifically required for cell cycle progression [62] [63] **(Fig. 9).**

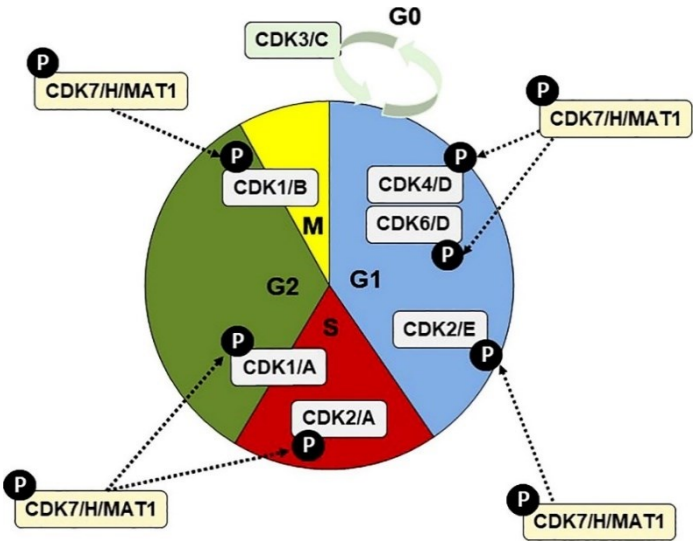

Figure 9 Schematic illustration of the regulation of cell cycle progression by cyclin/CDKs complexes.

CDKs activity requires binding to specific cyclins. However, there are other factors modulating the activity of this complex including [63]:

- the presence of CDK inhibitors, also known as CKI (Cyclin-Dependent Kinase Inhibitors) and referred as the "brakes" of the cell cycle,
- the phosphorylation state of CDK itself [52].

CDKs are highly conserved protein kinases that phosphorylate serine and threonine residues on proteins. Mammals contain thirteen CDKs, seven of which are involved in cell cycle regulation: CDK1, 2, 3, 4, 6, 7, 8. A complex mechanism of activation controls the activity of CDKs through the binding of CDK to a regulatory component known as "cyclin"[64].

Cyclins form a complex with CDK, which begins to activate but also requires phosphorylation for full activation. The formation of a complex activates the CDK active site. Cyclins do not have an enzymatic activity but have binding sites for certain substrates and drive CDKs to subcellular locations. Due to their essential functions in the regulating of the cell cycle and transcription, CDKs have been identified as interesting therapeutic targets for cancer and other disorders [53].

Several CDK inhibitors (CDKIs) have been generated and tested in multiple clinical studies for various tumor types over the past 20 years [65].

CDKIs are divided into:

• First generation CDKI

• Second generation CDKI

First generation of cyclin-dependent kinase inhibitors, later named "pan-CDKIs," were the first cyclin-dependent kinase inhibitors generated, but they did not achieve the expected clinical success [62]. Among these, flavopiridol (1, Fig 10) and (R)-roscovitine (2, Fig. 10) generated sufficient interest for clinical testing but the results showed toxicity and minimal efficacy.

Subsequently, these inhibitors were improved by synthesizing additional ones in an effort to increase their selectivity for cancer cells. Some of these second-generation drugs have showed high clinical success. The 2015 regulatory approval of the CDK4/6 inhibitor palbociclib (3, Figure 10) is a landmark [65]. Since then, two more CDK4/ 6 inhibitors, ribociclib (4, Fig. 10) and abemaciclib (5, Fig. 10), have been developed [65].

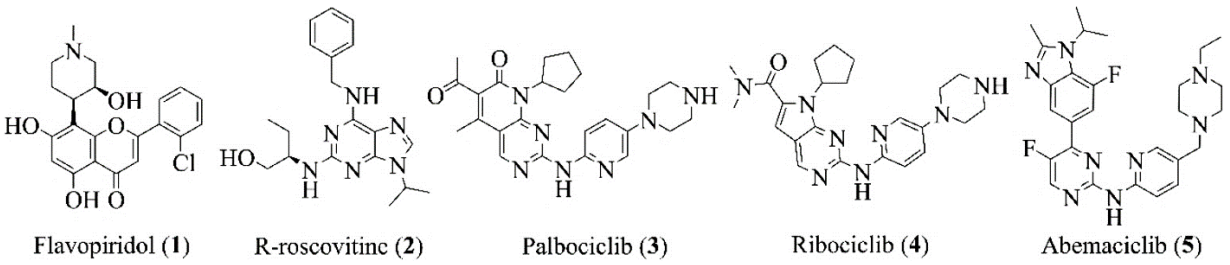

Figure 10 CDK inhibitors

1.12 Abemaciclib

Abemaciclib is a cyclin-dependent kinase (CDK) 4 and 6 inhibitor, which blunt CDK4/646-mediated phosphorylation of RB1/p105 and affect the transition from G1 to S phase of the cell cycle [66].

Abemaciclib targets the proliferative activity of the cyclin D-associated kinases to induce cell-cycle exit in Rb-positive tumor cells but are mostly inactive in Rb-negative cells. Although this indicates that Rb is the only significant substrate, it is possible that other substrates of these kinases contribute to phenotypes after the cell cycle has ended. Understanding the effects of growth arrest induced by CDK4/6 inhibitors and how signaling pathways contribute to maintaining quiescent cells may be the key to improving combination therapies [67].

Abemaciclib got FDA approval as monotherapy or in combination with fulvestrant or hormone receptor (HR)-positive aromatase inhibitor for patients with metastatic breast cancer based on findings from the MONARCH-1–2–3 trials [68].

The liver enzyme CYP3A4 primarily metabolizes the drug to N-deethylabemaciclib (M2) and, to a lesser extent, hydroxyl derivatives (M18, M20) and an additional oxidative metabolite (M1). The

plasma protein binding rates of these metabolites are comparable to those of the parent substance [69].

Abemaciclib is primarily eliminated in the feces (81%) and to a smaller level in the urine (3%). The average elimination half-life is 18.3 hours [69].

Among developing therapeutics, inhibitors of cyclin-dependent kinase 4/6 (CDK4/6) have been identified as the most promising. The important roles of CDK4/6 in cell cycle regulation make these kinases effective therapeutic targets for the treatment of cancer. Abemaciclib, in combination with palbociclib and ribociclib, addresses an urgent unmet need for patients with HR+/HER2- metastatic breast cancer and provides a more effective chemotherapeutic option [69]. In addition, the capacity to cross the blood-brain barrier and the possible synergy between abemaciclib and immunotherapy are advantageous characteristics that give the opportunity for more successful multiple combination therapies [68].

Abemaciclib demonstrated 14 times higher inhibitory activity on cyclins D1/CDK 4/6 and D3/CDK than the other two inhibitors.

2. AIM

Malignant mesothelioma (MM) is an asbestos-related aggressive tumor with a median survival of 12 months. Mesothelioma cases continue to grow due to a long latency period 20-50 years between exposure and mesothelioma development. Multiple novel targets and pathways of interest have been identified from genomic studies of MM, but no predictive subsets or markers have been identified to help with patient selection and treatment. MM has therefore limited therapeutic options with minimal new therapy approvals in the past 15 years. Thus, there is still an unmet need for the identification of novel targets to improve therapy. Previous work from our laboratories have demonstrated that RB family members play an important role in regulating apoptosis in MPM cells. Thus, the Aim of this theses was to determine whether CDK4/6 inhibition would affect MPM biological responses and whether RB proteins might play a role in regulating the effect of CDK inhibitors.

We propose to:

AIM 1: Characterize the efficacy of CDK4/6 inhibitors in regulating growth and spheroids formation in MPM cells.

AIM 2: Define the mechanisms by which CDK4/6 inhibitors work and determine whether CDK4/6 inhibition could overcome cisplatin-resistance in MPM cells.

These experimental approaches have the potential to identify nocel mechanisms contributing to MPM cancer progression and open new avenue for therapy.

3. MATERIAL AND METHODS

3.1 Cell Lines and Culture Conditions

Mesothelioma and Mesothelium cell lines:

NCI-H28, NCI-H2452, MMB, ISTMES-2, MSTO-211H, NCI-H2052 mesothelioma cell lines and MET-5A immortalized normal mesothelial cells were purchased from American Type Culture Collection ATCC). ISTMES-2 were purchase from the ISTGE cell repository.

NCI-H28, NCI-H2452, MSTO-211H, NCI-H2052 cells were grown in RPMI-1640 supplemented with 10% fetal bovine serum (FBS), 1% penicillin-streptomycin, and 1% glutamine.

ISTMES –TWO were grown in DMEM and MMB in F12 both supplemented with 10% fetal bovine serum (FBS), 1% penicillin-streptomycin, and 1% glutamine.

MET-5A cells were grown in Medium 199 with 10% FBS, 0.5% penicillin-streptomycin, 1% glutamine, and 3.3 nM epidermal growth factor, 400 nM hydrocortisone, and 870 nM insulin. Cells were maintained in a humidified incubator set at 37°C and 5% CO2. Cells undergoing exponential growth were used for all the experiments. All cell culture reagents were purchased from Sigma Aldrich.

Silenced "protein pocket" cell lines:

To generate RB1/p105, RBL1/p107 and RBL2/p130 silenced cells, HEK-293FT cells were transfected with PAX2 packaging plasmid, PMD2G envelope plasmid, and pLKO.1.

The pLKO.1 vectors were used: expressing a shRNA targeting the human RB1/p105, RBL1/p107 and RBL2/p130

mRNAs and Scrambled shRNA (pLKO.1 shSCR, gift from S. Stewart, Addgene plasmid #17920). Following transfection, supernatants were collected, filtered and used for transducing MPM cells. Three days' post infection, cells were selected with 2 μg/ml puromycin (Sigma-Aldrich).

Cisplatin-resistant cell lines:

MSTO-211H and NCI-H2052 resistant to cisplatin were generated by selecting MSTO-211H and NCI-H2052 cells after treatment induced 5 times in increased concentration of cisplatin 5μM, 10μM, 15μM, 20μM and 25μM 72 h, and then the treated cells grew in drug-free medium for 10 days. Another treatment was not administered until the cells were in exponential phase. The cells were maintained in RPMI-1640 supplemented with 20μM cisplatin (IC50), 10% fetal bovine serum (FBS), 1% penicillin-streptomycin, and 1% glutamine. Cells were kept at 37˚C in a humidified atmosphere of 5% CO2 and 95% air.

3.2 Cell Viability Assay

NCI-H28, NCI-H2452, MMB, ISTMES-2, MSTO-211H, NCI-H2052 mesothelioma cell lines and MET-5A immortalized normal mesothelial cells were seeded in triplicates in 96-well plates at a density of 800 cells/well for MSTO-211H and 1200 cells/well for the other cell lines and allowed to adhere for 24 h. Cells were then treated with palbociclib, ribociclib and abemaciclib at doses ranging from 1.56 μM to 50 μM l for 72h. At the end of the treatment the

cells' viability was evaluated by MTS assay (CellTiter 96® AQueous One Solution Cell Proliferation Assay, Promega, Milan, Italy), following the manufacturer's instructions. The percentage of cell viability was calculated assuming as 100% the number of untreated cells. The concentration of *CDKi* required to inhibit 50% of cell viability (half maximal inhibitory concentration, IC50) was determined by a dose-response curve by using GraphPad Prism 7 Software.

The three lines of MSTO-211H with retinoblastoma protein silenced plus scramble as control (RBL2/p130, RBL1/p107 and RB1/p105 and Scramble) were seeded in triplicates in 96-well plates at a density of 1200 cells/well and allowed to adhere for 24 h. Cells were then treated with abemaciclib at doses ranging from 0.3 μM to 4.8 μM l for 72h. At the end of the treatment the cells' viability was evaluated by MTS assay (CellTiter 96® AQueous One Solution Cell Proliferation Assay, Promega, Milan, Italy), following the manufacturer's instructions. The percentage of cell viability was calculated assuming as 100% the number of untreated cells. Statistical analysis was carried out by applying the unpaired Student's t-test. Statistically significance was settled at * $p < 0.05$, ** $p < 0.005$ vs 0.

MSTO-211H and NCI-H2052 cisplatin-resistant were seeded in triplicates in 96-well plates at a density of 1200 cells/well and 800cells/well respectively and allowed to adhere for 24 h. Cells were then treated with abemaciclib at doses ranging from 2 μM to 32 μM l for 72h. At the end of the treatment the cells' viability was evaluated by MTS assay (CellTiter 96® AQueous One Solution Cell Proliferation Assay, Promega, Milan, Italy), following the manufacturer's instructions. The percentage of cell viability was calculated assuming as 100% the number of untreated cells. Statistical analysis was carried out by applying the unpaired Student's t-test. Statistically significance was settled at * $p < 0.05$, ** $p < 0.005$ vs 0.

3.3 Clonogenic Assay

For the clonogenic assay, 200 cells were seeded in each well of 6 well plates and, 24 h after seeding, they were treated with abemaciclib for 48 h at IC50 for each cell line. After 10 days, colonies were fixed with methanol and stained at room temperature for 30 min with crystal violet (Sigma-Aldrich).

3.4 Spheroids generation

Spheroid formation was performed in RPMI-1640 supplemented with 10% fetal bovine serum (FBS), 1% penicillin-streptomycin, and 1% glutamine. All cell culture reagents were purchased from Sigma Aldrich.

Spheroid formation was performed comparing two protocols: the Multiple Spheroid Protocol and the Single Spheroid Protocol

Single Spheroid Protocol

Spheroids were freshly prepared from the adhesion cultures three days (72 h) before each experiment. On the day of seeding (day 0), cells were detached with trypsin-EDTA as usual and centrifuged at 290× g for 5 min. Next, the pellet was resuspended in RPMI-1640 medium (with supplements), and cell counting was performed using a Burker chamber. After that, the cells were seeded in U-bottom Ultra Low Attachment (ULA) 96-well Microplates (Corning B.V. Life Sciences, Amsterdam, The Netherlands) at a density of 0.5×10^4 cells/well in 100 µL/well. After seeding, the U-bottom ULA 96-well Microplates were centrifuged at 340× g

for 30 min to foster cell aggregation. Next, the plate was incubated for up to 4 days at 37° C in a humidified atmosphere of 5% CO_2 during spheroid formation.

Multiple Spheroid Protocol

Three days (72 h) prior to each experiment, spheroids were freshly produced from the adhesion cultures. On the day of seeding (day 0), cells were detached using trypsin-EDTA and centrifuged for 5 minutes at 290 g. Next, the pellet was resuspended in RPMI-1640 media (with supplements), and a Burker chamber was used to count the cells. The cells were then seeded at a density of $3x10^4$ cells/well in 2000 L/well into Ultra Low Attachment (ULA) 6-well plates (Corning B.V. Life Sciences, Amsterdam, The Netherlands). During spheroid development, the plate was incubated for up to 5 days at 37° C in a humidified environment containing 5% CO_2.

Second-generation Spheroid Protocol

After multiple spheroids were create (day 5) they were broken using trypsin-EDTA for 5/10 minutes gently pipetting to separated single cells and centrifuged for 5 minutes at 290 g. After resuspending the pellet in RPMI-1640 medium (with supplements), the cells were counted using a Burker chamber. The cells were subsequently plated in Ultra Low Attachment (ULA) 6-well plates at a density of 3x104 cells/well in 2000 L/well (Corning B.V. Life Sciences, Amsterdam, The Netherlands). During spheroid growth, the plate was incubated for up to 4 days at 37° C in a humid atmosphere containing 5% CO_2.

3.5 Western Blotting Analysis

For total protein extraction, cells were lysed on ice for 30 min in a buffer consisting of 50mMTris-HCl pH 7.5, 1 mM EDTA pH 8.0, 150 mM NaCl, 1% NP-40, supplemented with protease and phosphatase inhibitor cocktails (Roche, Basilea, Switzerland). The protein samples were resolved by SDS-PAGE and blotted onto nitrocellulose membranes, which were then incubated with antibodies against RBL2/p130 (abcam cat# ab183039), phosphoRBL2/p130 S941 (custom by Covalab, Villeurbanne, France), phosphoRBL2/p130 S639 (Santa Cruz cat# sc16301) RBL1/p107 (cell signaling), phosphoRBL1/p107 S975 (Mybiosource cat# MBS9214765), RB1/p105 (cell signaling), phosphoRB1/p105 S780 (cell signaling # 9308), AKT(pan)(C67E7) (Cell Signaling cat# 4691), phosphoAKT S473 (Cell Signaling cat# 9271), Cyclin D1 (Cell Signaling cat# 2922), c-Myc (Cell Signaling cat# 9402), p21 waf1/cip1 (Cell Signaling cat# 294), p53(1C12) (Cell Signaling cat# 2524), CDK6 (B-10) (Santa Cruz cat#sc7961), CDK4 (B-10) (Santa Cruz cat# sc166373), MDM-2 (D1 V2Z) (Cell Signaling cat# 86934). After incubation with horseradish peroxidase-conjugated secondary antibodies, signals were detected through ECL (Amersham Biosciences, GE Healthcare, Little Chalfont, UK). The chemiluminescent images were analyzed by ImageQuant LAS 500 (GE Healthcare, Little Chalfont, UK).

3.6 Apoptosis Analysis

Apoptosis was assessed through flow cytometric analysis (BD FACSCalibur, Becton Dickinson BD Biosciences, Franklin Lakes, NJ, USA) of MPM cells treated for 48 h with abemaciclib at their IC50 values and stained with annexinV–FITC and propidium iodide (AnnexinV-FITC Kit, Biolegend, San Diego, CA, USA) according to the manufacturer's instructions.

3.7 Statistical Analysis

Statistical analyses were performed by Prism 7 (GraphPad software). Results were expressed as means ± standard deviation and derived from at least two independent experiments.

Statistical analysis was carried out by applying the unpaired Student's *t*-test. Statistically significance was settled at * $p < 0.05$, ** $p < 0.005$ vs 0. Data are presented as mean ± standard deviation of three different experiments ($n = 3$).

4. RESULT

4.1 Evaluation of the cytotoxic effects of new generation cyclin-dependent kinase (CDK) 4/6 inhibitors on MPM cell lines

To examine the impact of inhibiting Cyclin-Dependent protein kinases (CDKs) on pleural mesothelioma (MPM) cells, we treated a panel of MPM cell lines with three last generation CDK 4/6 inhibitors (CDKi): palbociclib, ribociclib, and abemaciclib. Specifically, we treated NCI-H28, IST-MES 2, NCI-H2452, MMB, MSTO-211H and NCI-H2052, which are representative of the three major MPM histotypes, with increasing concentrations of the three CDKi, ranging from 1.56 μM to 50 μM, and evaluate cell viability by MTS assay after 24h, 48h, and 72h of treatment. In addition, we tested the effectiveness of CDKi on an immortalized mesothelial cell line, MET-5A as control. Thus, we determined the IC50 values after 72h of treatment for all the MPM cell lines tested (**Table 1**).

Our data show that ribociclib and palbociclib only moderately reduced viability of MPM cell lines (**Fig. 11A, Fig. 11B**), while abemaciclib is showed cytotoxic effects on all MPM cell lines tested, including NCI-H2052, which are derived from the most aggressive sarcomatoid histotype. Moreover, abemaciclib did not determine the same toxic effects on the control mesothelial cell line, MET-5A (**Fig. 11C**). Being abemaciclib the most effective CDK 4/6 inhibitor on MPM cells, we used it for all subsequent experiments.

.

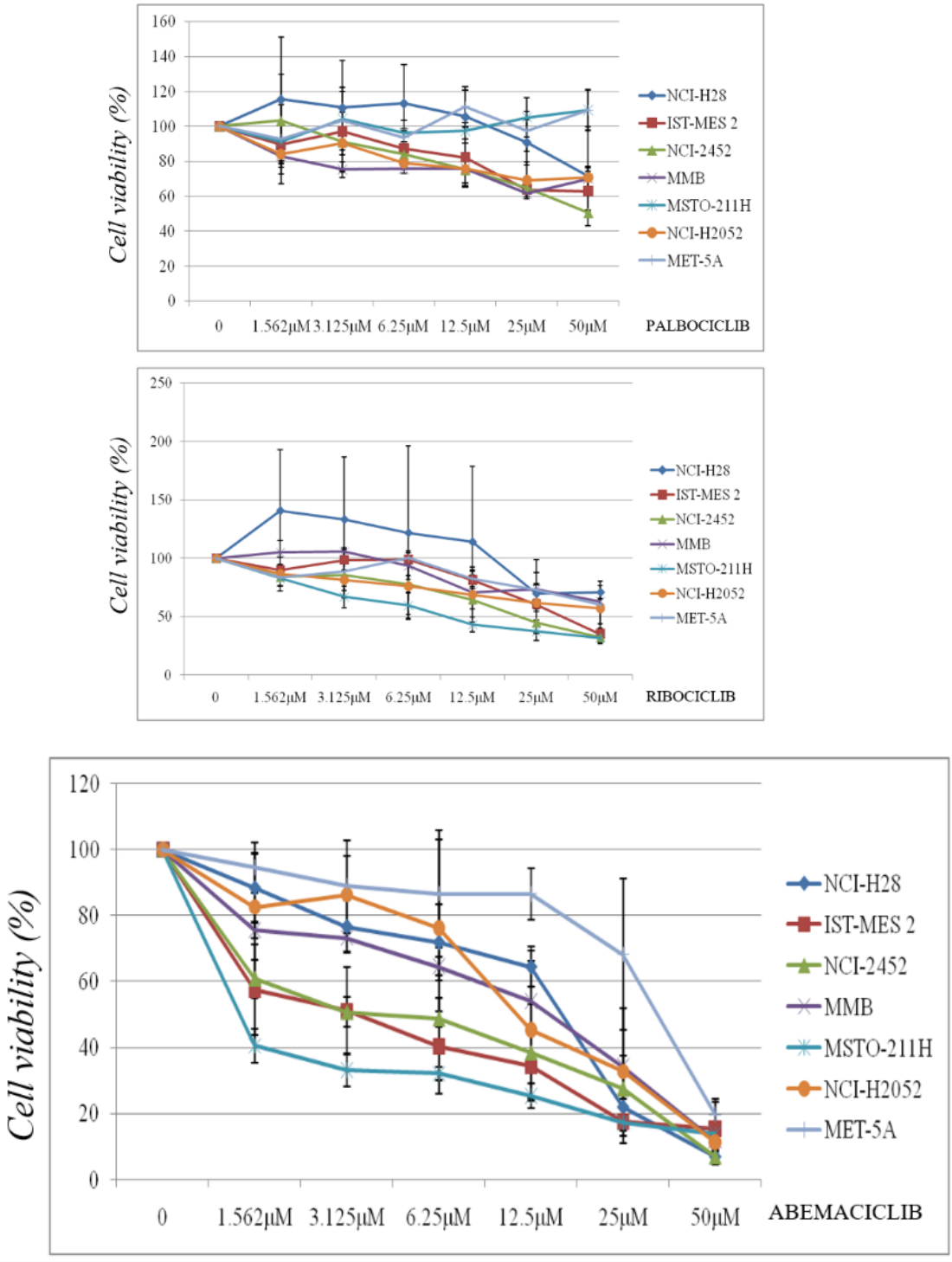

Figure 11: Effect of new-generation CDK inhibitors on mesothelioma cell viability. Dose–response growth curves with different doses of Palbociclib **(Fig. 1A)**, ribociclib **(Fig. 1B)** and abemaciclib **(Fig. 1C)** evaluated by MTS assay after 72 h of treatment of various mesothelioma cell lines (NCI-H28, IST-MES 2, HNCI-H2452, MMB, MSTO-211H, and NCI-H2052) cell lines and in immortalized normal mesothelial cells MET-5A. Experiments were repeated at least two times and results are expressed as mean ± standard deviation and expressed as percentages of cell viability (calculated in respect of control cells treated with DMSO alone).

CELL LINE	ABEMACICLIB IC50 (µM)	PALBOCICLIB IC50 (µM)	RIBOCICLIB IC50 (µM)
NCI-H28	11.61	ND	147
IST-MES 2	3.74	54.13	36.62
NCI-II2452	4.61	39.87	20.32
MMB	10.41	45.26	61.44
MSTO-211II	0.62	ND	10.51
NCI-H2052	1.07	59.28	36.11
MET-5A	31.59	ND	62.57

Table 1 IC50 values. Table shows the IC50 values for each cell line. IC50 values for some cell lines were not determined (ND) or were higher than the maximum dose used. The IC50 values were calculated using GraphPad Prism 5.01

4.2 Evaluation of long-term cytotoxic effects of abemaciclib on MPM cell lines

To determine whether abemaciclib inhibited long-term cell growth of MPM cells, we performed clonogenic assays. Interestingly, abemaciclib significantly inhibited colony formation of all MPM cell lines, including NCI-H2052, derived from the most aggressive mesothelioma histotype. **(Fig. 12).**

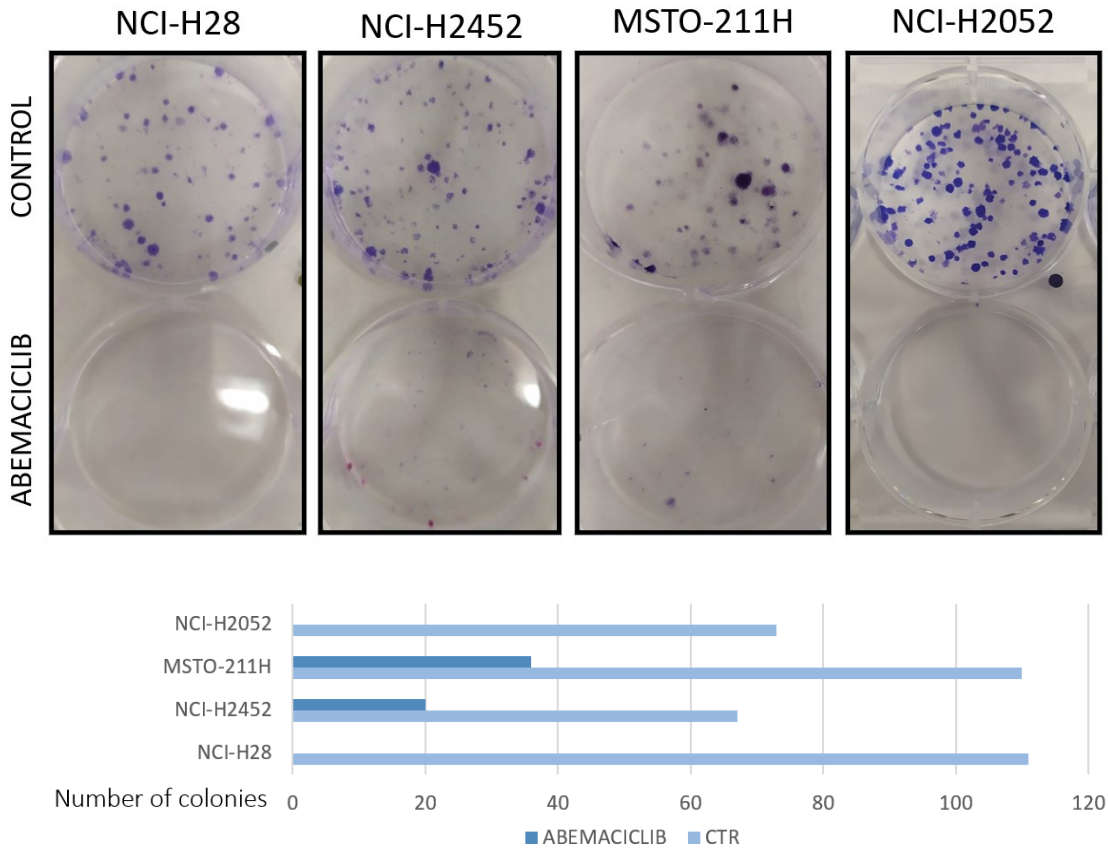

Figure 12 Long-term abemaciclib effects were assessed by clonogenic assay. Colonies were stained with crystal violet 10 days after a 48h treatment with abemaciclib (IC50). Representative plates from at least three independent experiments are shown.

Our data suggest that abemaciclib reduces the viability of MPM cells in short- and long-term cell growth at low doses. Thus, we decided to better understand the action of this drug on MPM cells, using different approaches.

4.3 MPM 3D-cell culture

4.3.1 Spheroids

Monolayer adherent cell cultures (also known as 2D culture) are the most common *in vitro* cell-based models. However, they are often less informative than the three-dimensional (3D) cell culture approach in mimicking the biological behavior of tumor cells, in particular the mechanisms leading to therapeutic escape and drug resistance [70]. So, we tested abemaciclib effects on both first and second generation MPM spheroids. For the approach of three-dimensional cultures in cancer drug development and target validation, we adopted ultra-low attachment (ULA) 96-well round bottomed plates, which, unlike conventional approaches, do not require coating to inhibit cell adhesion. Within 24 to 48 hours, tumour cell suspensions formed three-dimensional structures, which grow as single spheroid. at the center of the well [71] (**Fig. 13**).

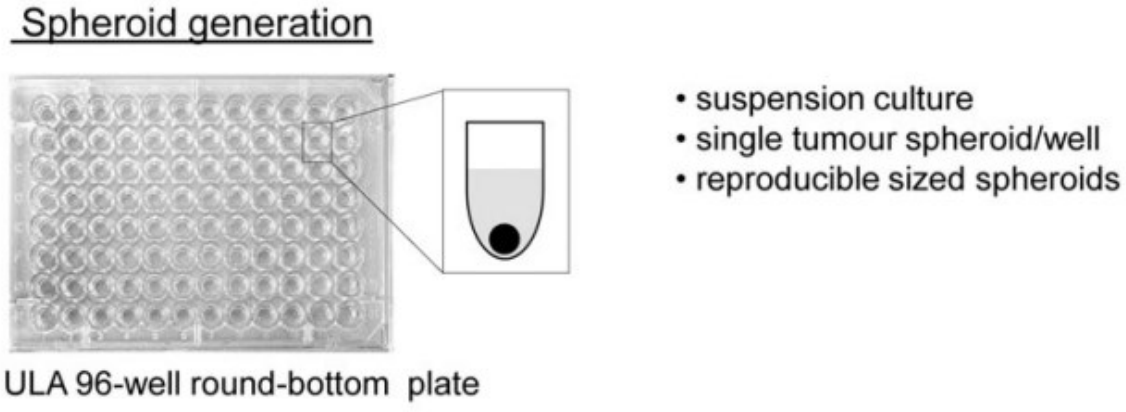

Figure 13 Ultra-low attachment (ULA) 96-well round bottomed plate

We tested then the ability of four mesothelioma cell lines (NCI-H28, NCI-H2452, MSTO-211H and NCI-H2052) to grow as spheroids for 4 days **(Fig. 14)**. Interestingly, all the MPM cell lines formed spheroids without the addition of any supplements.

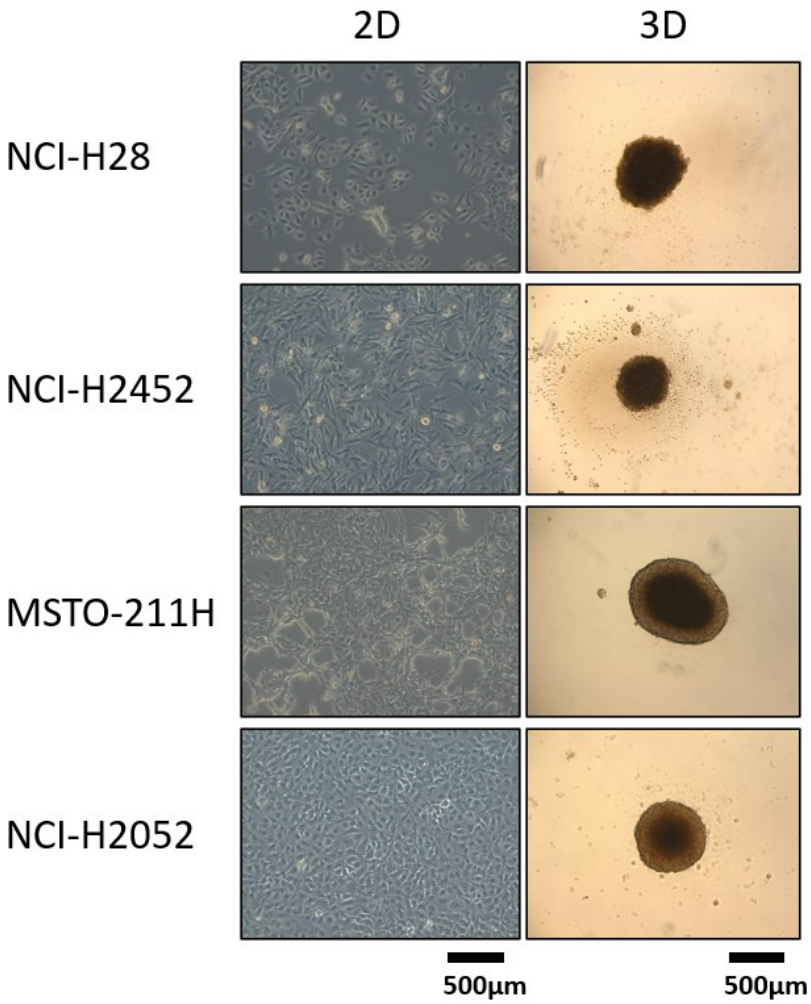

Figure 14 MPM cell lines in 2D and 3D culture. Monolayer cells were seeded in a 100mm cell culture dish. Ultra-low attachment (ULA) 96-well plates were used to generate suspension cultures of reproducibly sized, single spheroids in each well in RPMI medium (+10%FBS, +1% L-Glu), at a density of 0.5×10^4 cells/well in 100 µL/well of medium. After the seeding, the microplates are centrifuged at 340× g for 30 min, as described in more detail in Material and Method section. The plate is incubated at 37 ◦C in a humidified atmosphere of 5% CO2 during spheroid formation. The use of ULA U-bottom microplates combined with plate centrifugation after plating facilitates cell aggregation in a round shape, causing the formation of a single spheroid/ well. Images were acquired 4 days after seeded.

Our results show that cells derived from the epithelioid histotype (NCI-H28, NCI-H2452) were slower in forming single-spheroid, which was also smaller when compared to to the biphasic (MSTO-211H) and sarcomatoid histotype-derived cells (NCI-H2052), which developed bigger spheroids after 4 days and we could also clearly recognize the necrotic core in the middle of MSTO-211H and NCI-H2052 spheroids.

4.3.2. Abemaciclib inhibits the MPM spheroids formation

We then decided to test wherever abemaciclib inhibited spheroid formation in MPM cells. We tested the ability of MPM cells (NCI-H28, NCI-H2452, MSTO-211H, NCI-H2052) to grow as spheroids media supplemented or not with abemaciclib for 4 days. Notably, abemaciclib at low concentration (5uM) significantly inhibited the ability of MPM cells to generated spheroids (**Fig. 15**).

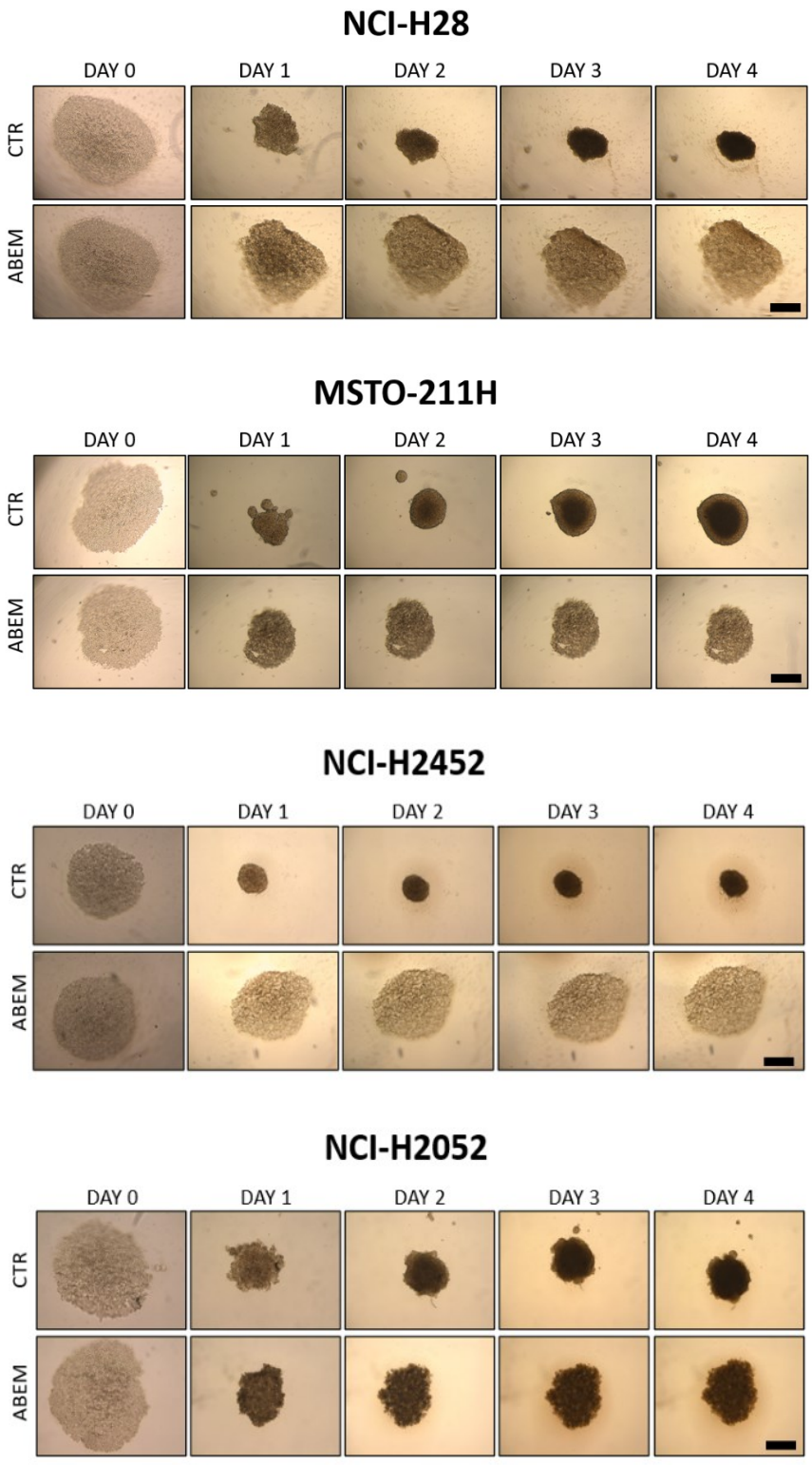

Figure 15 MPM Single Spheroids treated with abemaciclib at day 0. Cells were seeded at a density of 0.5 x 104 cells/well in U-bottom ULA 96 well plates and supplemented with abemaciclib (5µM) or DMSO, as a control, at day 0. Images were acquired at day 0, day 1, day 2, day3 and day 4. Scale bar: 500 µm. All experiments were performed at least three times.

Because 3D cell culture is better recapitulated *in vivo* tumours than 2D cells, our data suggest a that abemaciclib could be effective in inhibiting MPM.

4.3.3. Completely formed spheroids treatment with abemaciclib

Because we demonstrated that abemaciclib blocked the formation of spheroids, we studied the impact of abemaciclib on 2-day-old spheroids, to determine whether the drug reached sufficient concentrations to provide an antitumor effect on target cells of already formed spheroids.

Two days later, when spheroids were fully developed, we treated them with abemaciclib for additional 48 hours. As shown in **Figure 16**, in presence of abemaciclib spheroids generated from the epithelioid histotype (NCI-H28 and NCI-H2452) lost their integrity and were not as compact as compared to spheroids growing in media without the inhibitor **(Fig. 16A, Fig. 16B).** In contrast, the spheroids formed from biphasic (MSTO-211H) and sarcomatoid (NCI-H2052) histotypes showed a drastically increased circumference of the necrotic core and the overall volume decreased as the prefoliation area was severely reduced **(Fig. 16C, Fig. 16D)**

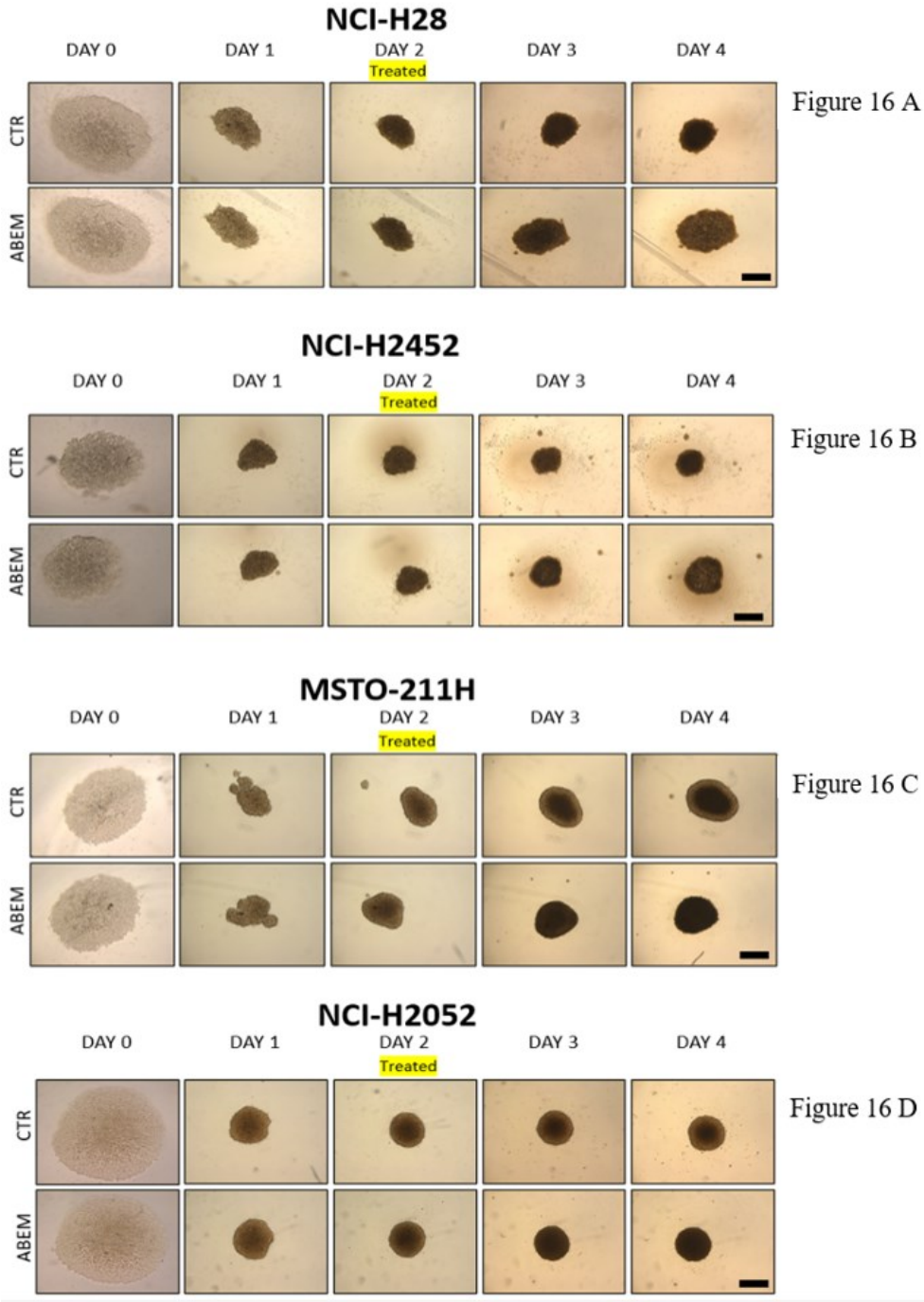

Figure 16 MPM 2-days-old spheroids treated with abemaciclib. Cells were seeded at a density of 0.5 x 10^4 cells/well in U-bottom ULA 96 well plates., After 2 days were treated with abemaciclib (10 μM) or DMSO as control. Images were acquired at day 0, day 1, day 2(day of treatment), day3 and day 4. Scale bar: 500 μm. All experiments were performed at least three times.

4.3.4. Second-generation spheroids

To confirm the ability of abemaciclib to penetrated deeply in the 3D cell structure and ~~d~~ reach all cells of the multicellular structured spheroid, we seeded 30,000 cells/mL in full media in 6 wells ultra-low attachment plate and when the spheroids were completely formed (day 2), we treated them with 5uM abemaciclib for 72 hours, same concentration that was able to block the formation of the first-generation spheroids. After that, we broke the spheroids with trypsin and seeded cells again to obtain second-generation spheroids. Abemaciclib likely reached deeply inside the spheroid, as in fact abemaciclib significantly inhibited the ability of all MPM cell lines to form second-generation spheroids **(Fig. 17).**

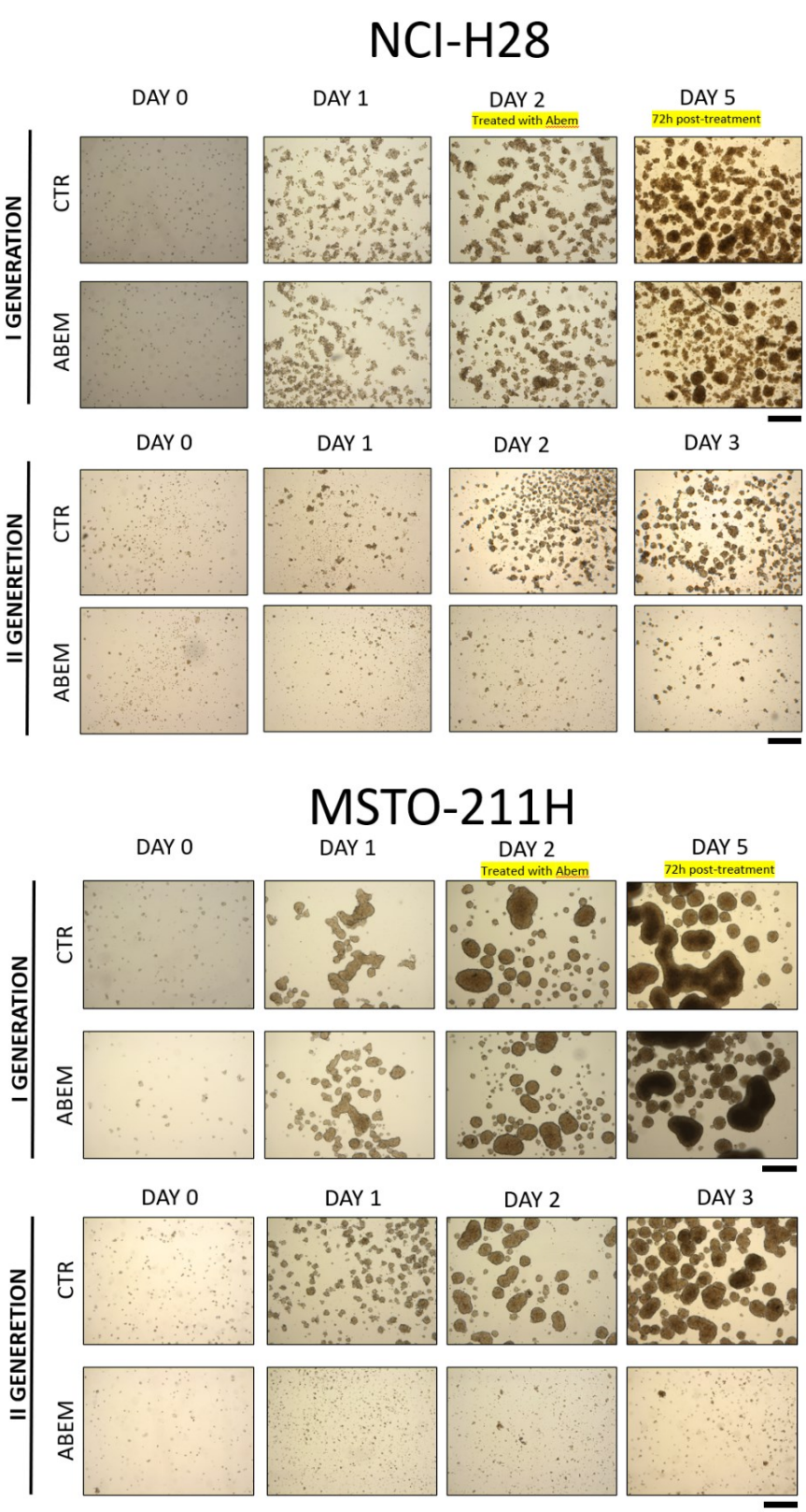
NCI-H28
DAY 0
DAY 1
DAY 2
Treated with Abem
DAY 5
72h post-treatment
I GENERATION
CTR
ABEM
DAY 0
DAY 1
DAY 2
DAY 3
II GENERETION
CTR
ABEM
MSTO-211H
DAY 0
DAY 1
DAY 2
Treated with Abem
DAY 5
72h post-treatment
I GENERATION
CTR
ABEM
DAY 0
DAY 1
DAY 2
DAY 3
II GENERETION
CTR
ABEM

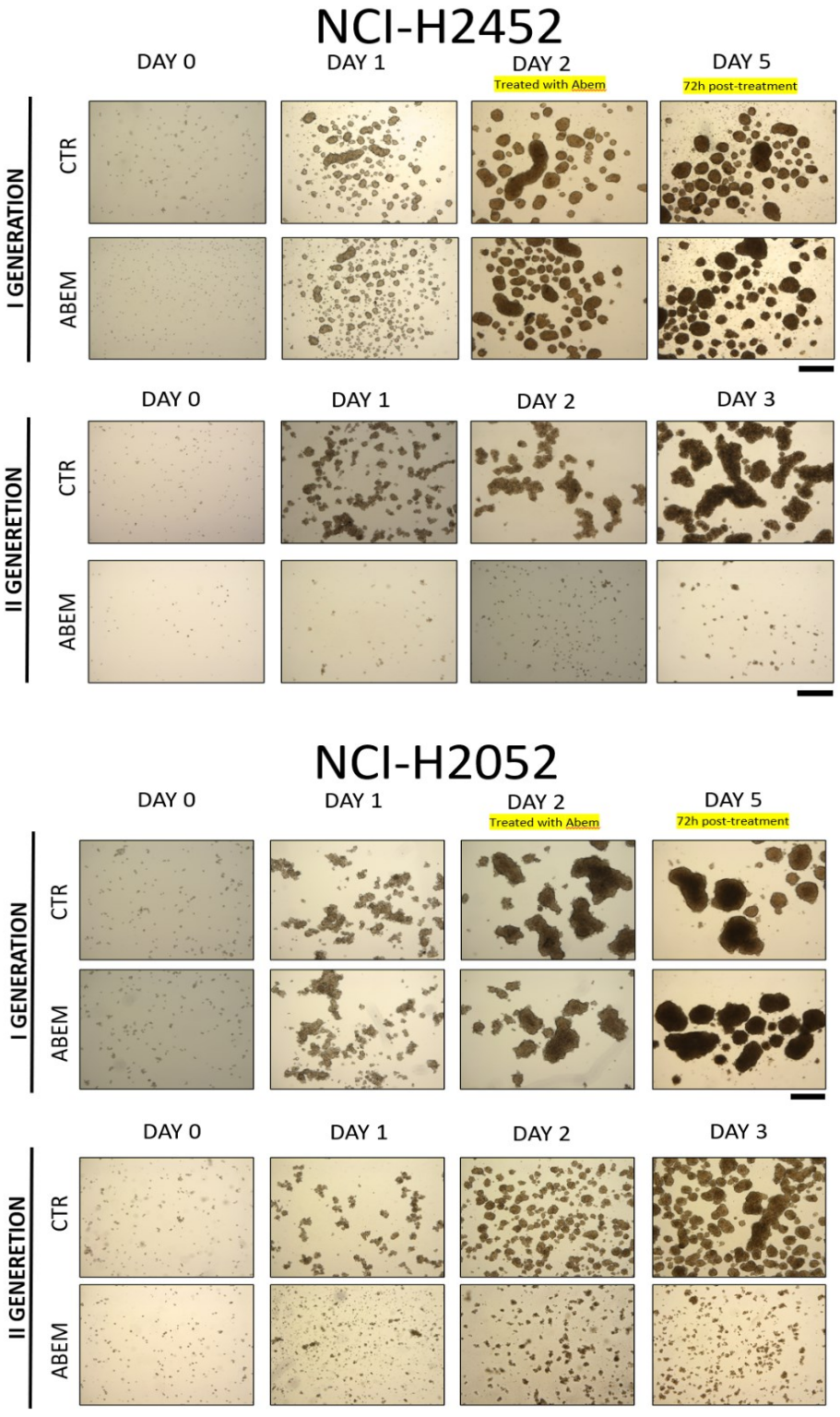

Figure 17 Cells were seeded at a density of 30 x 10^4 cells/well in 3mL of RPMI medium (+10%FBS, +1%L-Glu) in ULA 6 well plates. After 2 days were treated for 72 hours with abemaciclib or DMSO as control. Spheroids were washed with PBS 1X and incubated with trypsin for 5 min to break the spheroid in single cells and seeded again as the first step and growth monitored. Images were acquired at day 0, day 1, day 2(day of treatment), day 5 and day 1, day 2 and day 3. Scale bar: 500 µm. Scale bar: 500 µm.All experiments were performed at least three times.

Collectively, our findings demonstrate that abemaciclib blocks the formation of first- and second-generation spheroids formed by MPM cells and decreases cell proliferation of 3D cell cultures.

4.5 Abemaciclib induces cell death in MPM cell lines

At this point, in order to characterize the pathways by which abemaciclib induced cell death, we performed a cytofluorimetric assay to assess annexin levels after 48 hours treatment with abemaciclib (IC50). Annexin V and propidium iodide staining are commonly used to determine apoptotic cell death. Annexin V it is a human vascular anticoagulant, a Ca2+-dependent phospholipid-binding protein with a high affinity for the anionic phospholipid phosphatidylserine (PS). PS is situated on the cytoplasmic surface of the plasma membrane in healthy cells. However, during apoptosis the plasma membrane undergoes structural changes, including the translocation of PS from the inner leaflet (intracellular side) to the outside leaflet (extracellular side) of the plasma membrane. Propidium iodide, on the other hand, has the capacity to bind to DNA and can only enter necrotic or late apoptotic cells.

As shown from the percentages of % early (only annexin-V positive cells) and late apoptosis (both annexin-V and PI positive cells) reported in Table2, abemaciclib induced apoptosis in the tumor lines tested without major effects on mesothelial cells. These results suggest that abemaciclb caused a programmed cell death in MPM cell lines but not in mesothelial cells.

Cell lines	% early apoptosis		% late apoptosis	
	DMSO	ABEMACICLIB	DMSO	AMEBACICLIB
NCI-H28	78,01 %	26,79 %	16 %	64 %
NCI-H2452	76,14 %	60,38 %	7,39 %	24 %
IST-MES 2	79,7 %	34 %	8,6 %	55 %
MET-5A	71,3 %	55,4 %	19,15 %	25,7 %

Table 2 Percentages of early and late apoptosis induced by 48h treatment with abemaciclib at the IC50 value. After treatment, the cells were analyzed by flow cytometry using the annexin-V assay and the percentage values represent the average of two experiments

4.6 Evaluation of abemaciclib modulation of cell cycle-related protein levels

To elucidate the molecular mechanism of abemaciclib action, we tested the phosphorylation and the expression of several cell cycle-related proteins, which are targeted by CDK complexes inhibited by abemaciclib, in a panel of MPM cells (NCI-H28, MSTO-211H and NCI-H2052).

First, we tested by western blotting analysis the baseline and phosphorylated expression of RB1/p105, RBL1/P107 and RBL2/P130. The expression of and RB1/p105 and RBL1/p107 was, as expected, dramatically decreased in NCI-H28 and NCI-H2052 cell lines, but not significantly affected in MSTO-211H cells. The levels of phosphorylated pRB1/pp105 (S780) and pRBL1/pp107 (S975) proteins was sharply reduced in all MPM histotypes (**Fig. 18**). Total levels of RBL2/p130 were not altered by abemaciclib treatment but the level of RBL2/p130

phosphorylation at S952 and S941 was significantly decreased (**Fig. 18**). These results suggest that abemaciclib differentially affects the expression and activation of RB protein family members. Accordingly, we demonstrated by immunoblot that abemaciclib treatment reduces these phosphorylation events and restore RBL2/p130, RBL1/p107 and RB1/p105 function [72] [73].

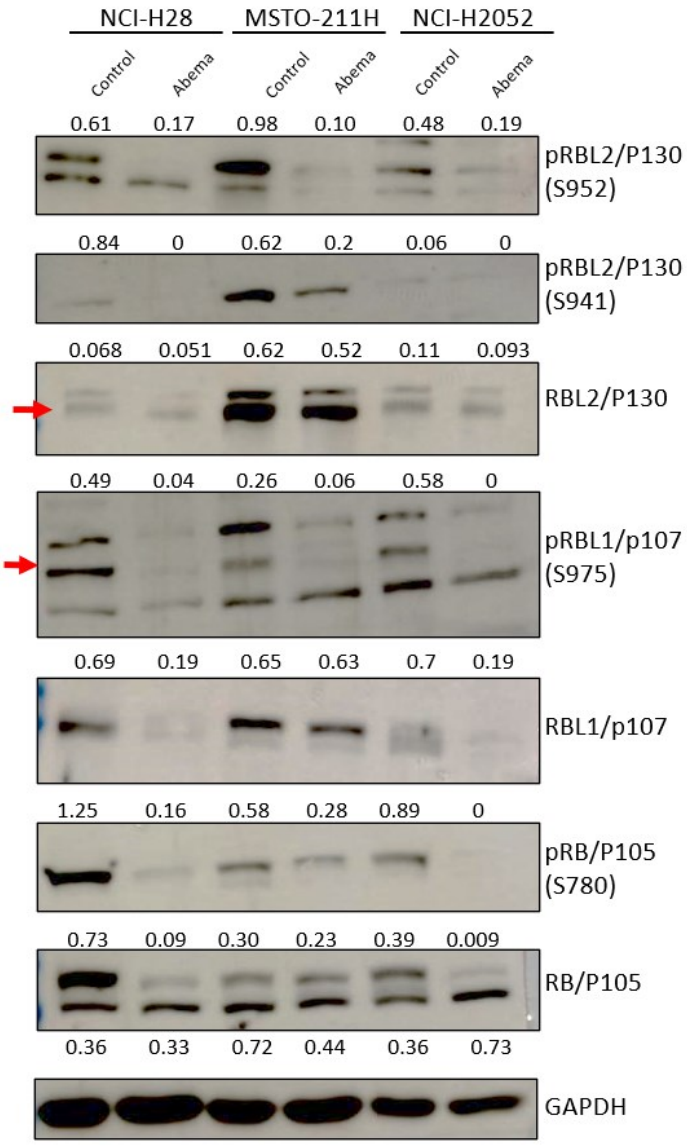

Figure 18. Effects of abemaciclib on Rb protein family. NCI-H28, MSTO-211H and NCI-H2052 cells were treated according to its respective IC50 value for 48 hours with abemaciclib and DMSO~~,~~ as ~~a~~ control. Analysis of total and phosphorylated levels of RBL2/p130, RBL1/p107 and RB1/p105 proteins were determinate by immunoblot. Arrows indicate bands corresponding to RBL2/p130, phosphorylated RBL1/p107(S975) and RB/p105. GAPDH was used as standard. Quantification was performed by densitometric analysis using ImageJ program. All experiments were performed at least 2 times.

To further define the mechanism of abemaciclib action, we examine whether the AKT pathway was affect after CDK 4/6 inhibitor treatment. Notably, abemaciclib effectively inhibited the AKT pathway after 48 hours of treatment, as demonstrated by the significant reduction of phosphorylated AKT levels in all MPM cells **(Fig. 19)**

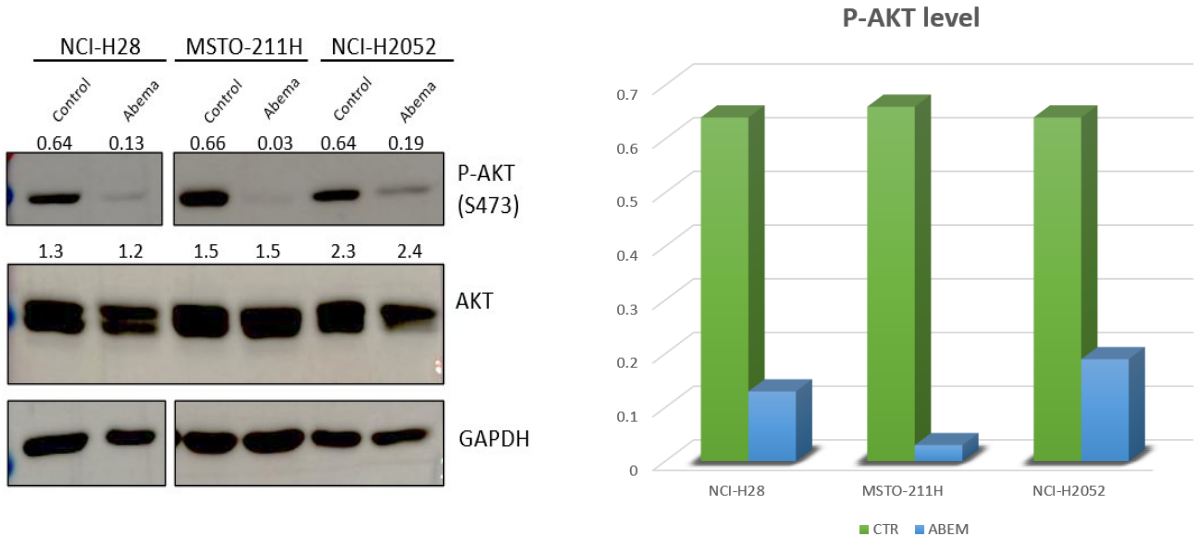

Figure 19 MPM cells NCI-H28, MSTO-211H and NCI-H2052 were treated for 48 hours with abemaciclib used at IC50 and DMSO, as a control. Levels of total and phosphorylated AKT were determinate by immunoblot. GAPDH was used as normalization control. Quantification was performed by densitometric analysis using ImageJ program. All experiments were performed at least three times.

We have recently demonstrated that in MPM cells RBL2/p130 is direct AKT targets and modulate the apoptotic process associated with AKT inhibition [59].

4.6 Role of pocket proteins in MSTO-211H cell line-response to abemaciclib

To better understand the molecular mechanism of abemaciclib action, we studied the role of pocket proteins and generated MSTO-211H cells were we stably depleted either RBL2/p130, RB1/p105 or RBL1/p107 by shRNA approaches. (**Fig. 20**)

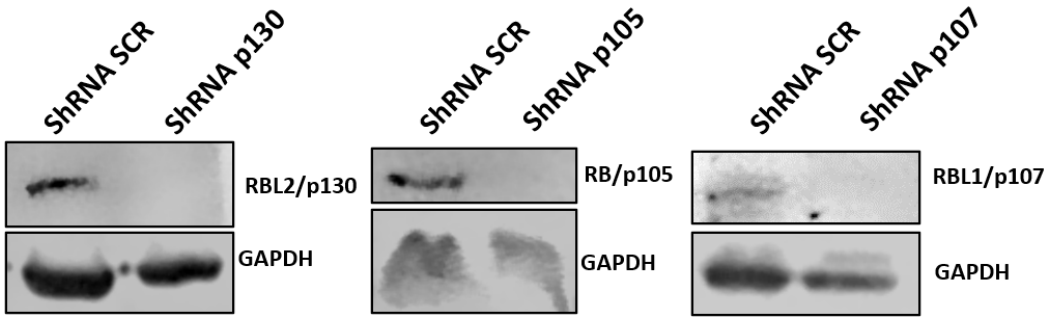

Figure 20 Pocket protein depletion in MSTO211-H cells. MSTO211-H cells singly depleted of- pocket protein were generated by shRNA approaches. Expression was assessed by immunoblot with specific antibodies. ShRNASCR are sh-control-transfected cells.

According to our previous data, the phosphorylation of all pocket proteins is downregulated after MPM cells were treated with abemaciclib. To study the role of these proteins during abemaciclib treatment, we exposed all MSTO-211H depleted cells and controls with increasing concentrations of abemaciclib ranging from 0.3 μM to 4.8 μM and evaluate cell proliferation by MTS assay after 72h of treatment. Abemaciclib did not significantly affect cell viability of MSTO-211H with p130 and p107 depletion, as compared to control lines (MSTO-211H shRNA SCR) but it reduces the viability in MSTO-211H with p105 depletion. (**Fig. 21).**

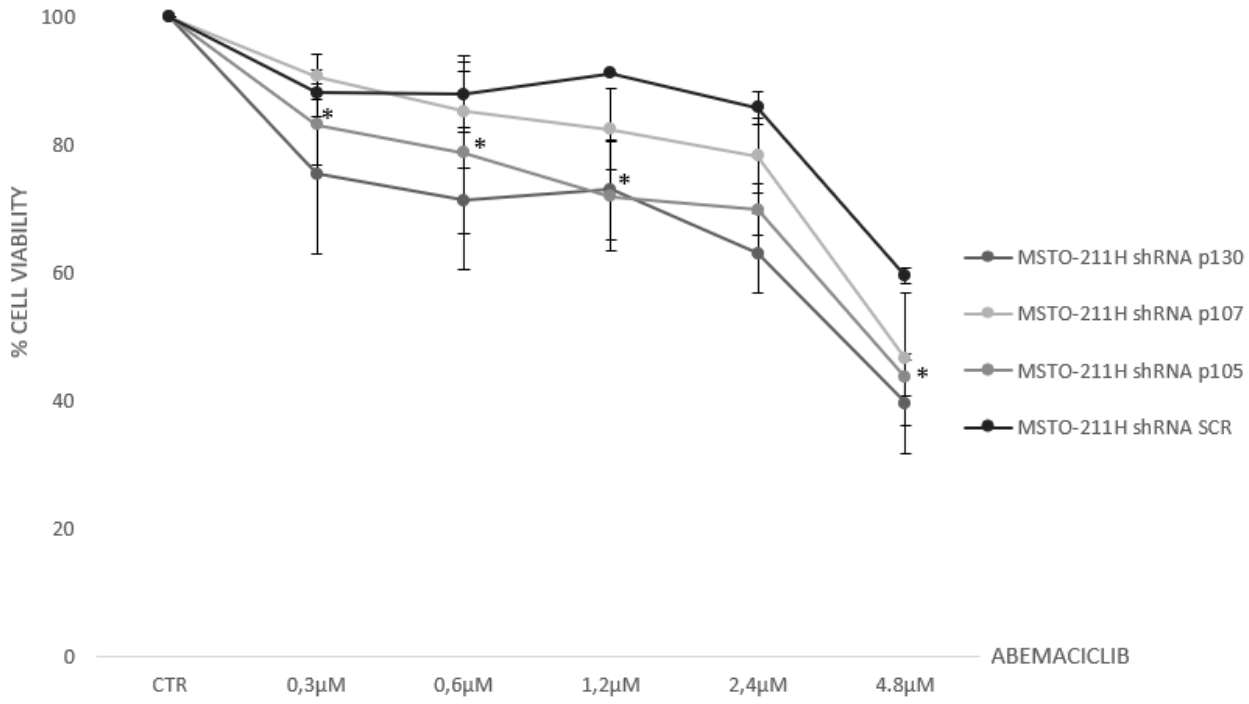

Figure 21 Effect of abemaciclib on pocket protein depletion in MSTO211-H cells viability. Dose–response growth curves with different doses of abemaciclib (0.3 µM, 0.6 µM, 1.2 µM, 2.4 µM, 4.8 µM) evaluated by MTS assay after 72 h of treatment pocket protein depletion in MSTO211-H cells. Statistical analysis was carried out by applying the unpaired Student's t-test. Statistically significance was settled at * $p < 0.05$, ** $p < 0.005$ vs control. Data are presented as mean ± standard deviation expressed as percentages of cell viability (calculated with respect to control cells treated with DMSO alone) of three different experiments (n = 3).

These very preliminary results suggest that RB1/p105 expression levels might affect MPM cell response to abemaciclib, response not affected instead by either p107 or p130.

4.7 Role of pocket proteins in spheroids formation

It has been demonstrated that the population of G0/G1 phase increased in the spheres (67 vs. 38%) as compared to monolayer cultures. Despite the absence of a substantial variation in stem cell surface markers (CD44, CD90, CD133, EpCAM, and ABCG2), sphere-forming cells exhibited a dramatic elevation of the CDK inhibitor p27 [74]. Thus, we decide to test whether pocket proteins can affect the capacity of MPM cells to form spheroids. However, as shown in **Figure 22,** we did not detect any difference between controls or pocket-proteins-depleted MSTO-211H cells in their ability to form spheroids as in fact we did not detect any difference in dimension, shape, and numbers. In addition, the perimeter of the necrotic and hypoxic core had the same circumference. Thus, based on the results we can deduct that pocket proteins are not important key regulators of spheroids formation in MPM cells.

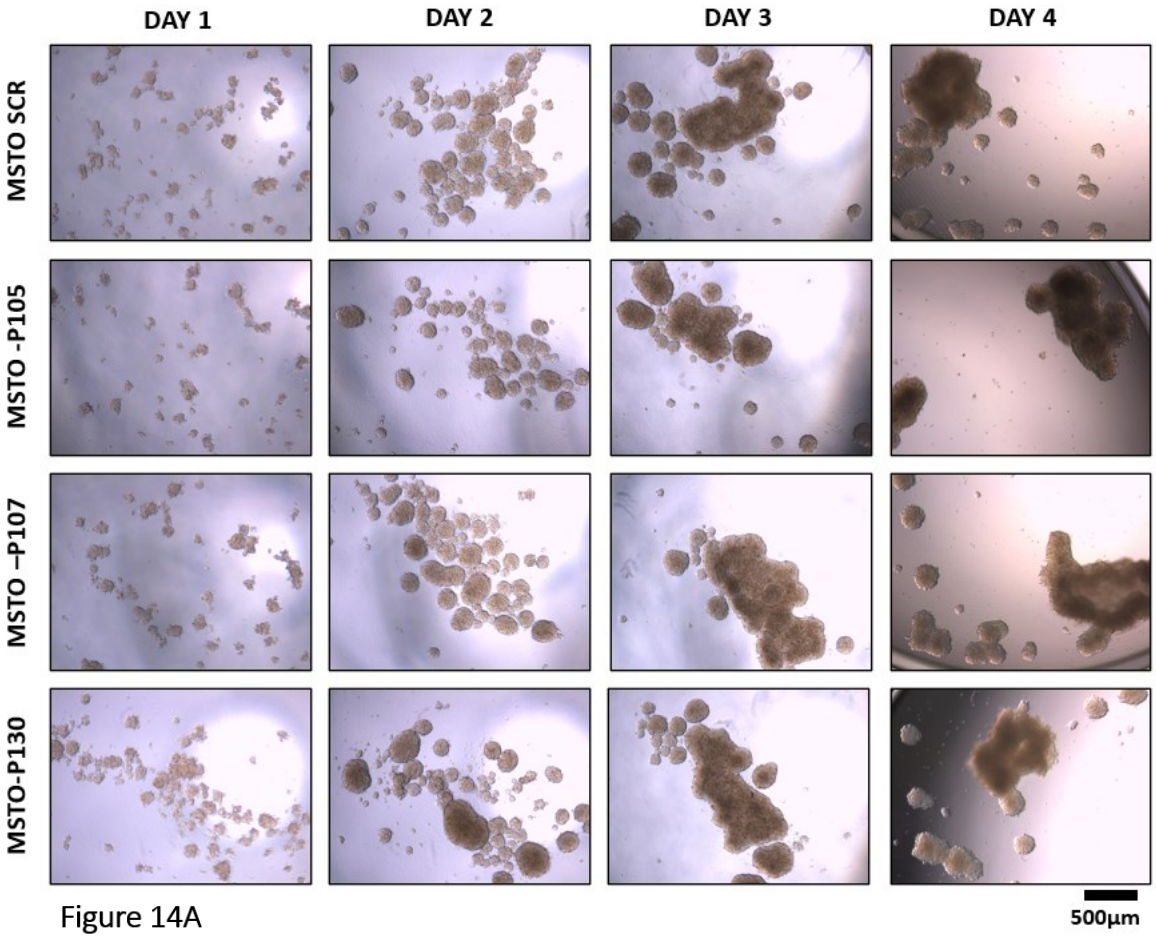

Figure 14A

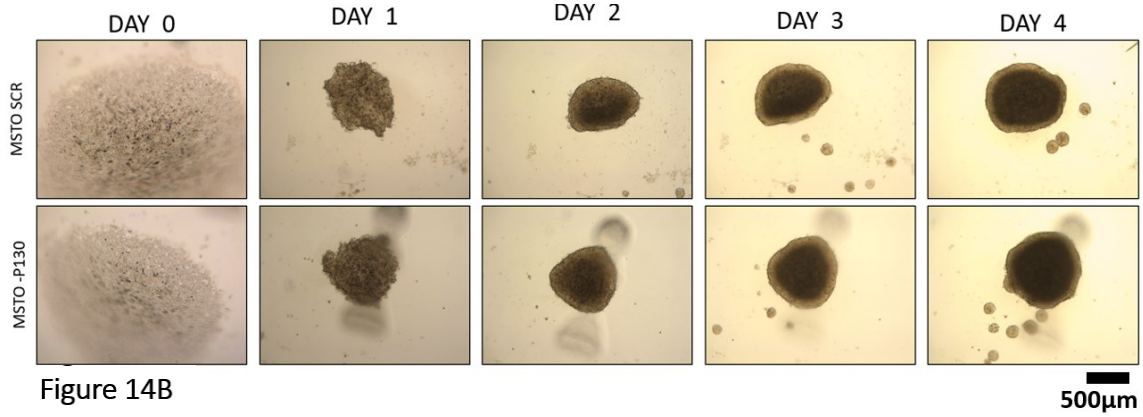

Figure 14B

Figure 22 Four days time-laps of spheroids with pocket protein depletion in MSTO211-H cells. Cells were seeded at a density of 30 x 10^4 cells/well in 3mL of RPMI medium (+10%FBS, +1%L-Glu) in ULA 6 well plates. Images were acquired at day 0, day 1, day 2, day 3 and day 4 (**Fig. 14A)**. Cells were seeded at a density of 0.5 x 10^4 cells/well in U-bottom ULA 96 well plates in 100 µL of RPMI medium (+10%FBS, +1%L-Glu). Images were acquired at day 0, day 1, day 2, day3 and day 4(**Fig. 14B**). Scale bar: 500 µm. All experiments were performed at least three times.

4.8 Cisplatin Resistance

Platinum(II) complexes such as cisplatin and carboplatin are clinically approved for MPM therapy often in combination with antimetabolites such as pemetrexed or gemcitabine [75]. However, severe side-effects and the insurgency of drug resistance limit the efficacy of cisplatin [75]. It has been observed that 50% of patients treated with cisplatin develop intrinsic resistance or acquire multidrug resistance rapidly [76].

We generated MSTO-211H and NCI-H2052 cell lines resistant to cisplatin to better understand the action of abemaciclib. We examined whether those cell lines resistant to cisplatin were instead sensitive to abemaciclib. We treated with abemaciclib for 72 hours at five different concentrations (2μM, 4 μM, 8 μM, 16 μM, 32μM) the two cisplatin-resistant cell lines and the respective parental cell lines as control and we evaluated the percentage of cell viability by MTS assay. Interesting at the concentration of 4 μM the biphasic histotype-derived cells resistant to cisplatin had developed a significative resistance to abemaciclib as well. In contrast cells derived from the most aggressive histotype did not show any differences between parental cell line and cisplatin-resistant cell line.

This data suggests that abemaciclib could be an effective and an important antitumoral drug to that patients who have develop a cisplatin resistant. (**Fig. 22**).

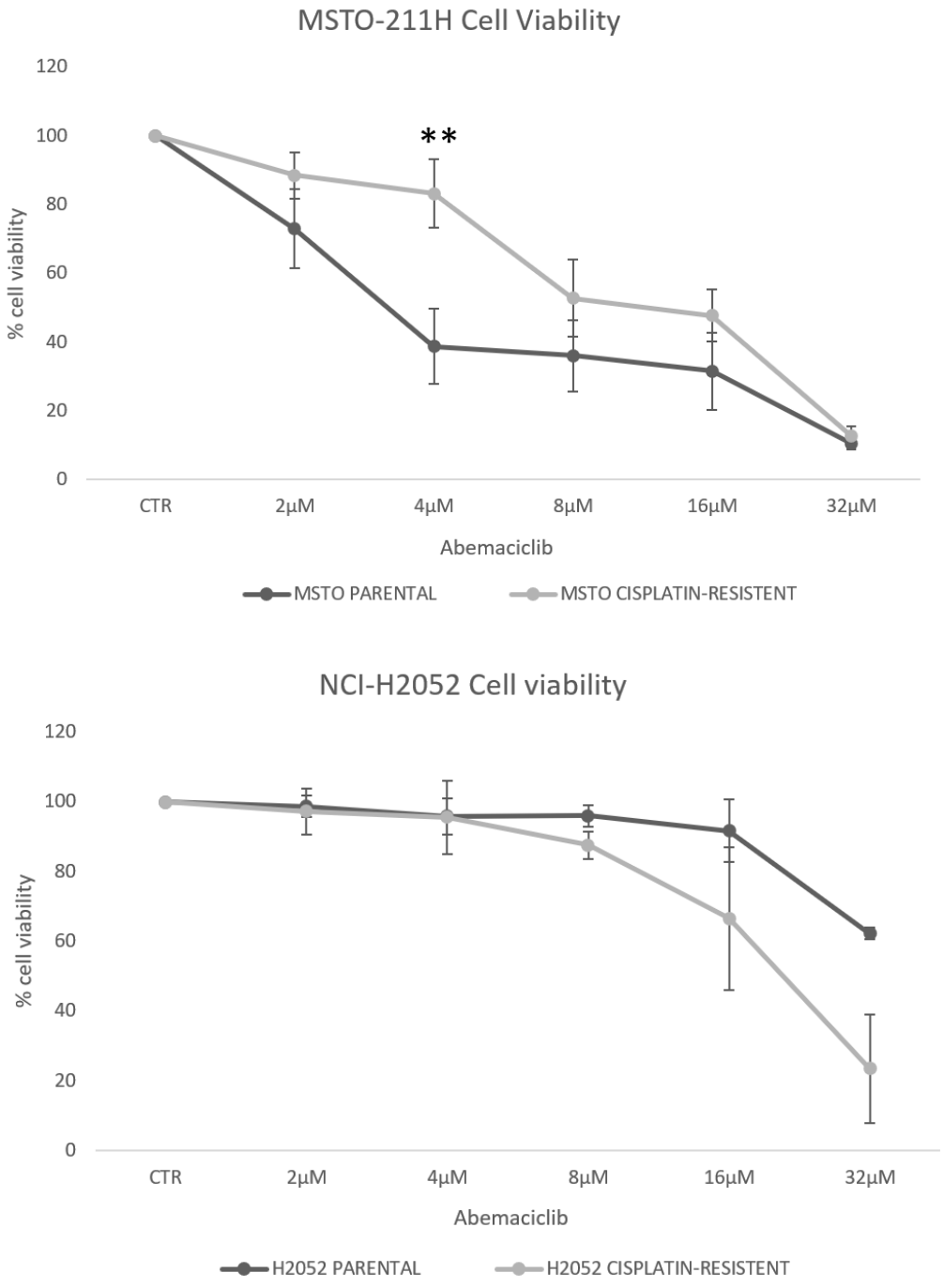

Figure 22 Effect of abemaciclib on NCI-H2052 and MSTO-211H cisplatin-resistant cell viability. Dose–response growth curves with different doses abemaciclib evaluated by MTS assay after 72 h of treatment of NCI-H2052 and MSTO-211H cisplatin-resistant cell. Statistical analysis was carried out by applying the unpaired Student's t-test. Statistically significance was settled at * $p < 0.05$, ** $p < 0.005$ vs control. Data are presented as mean ± standard deviation expressed as percentages of cell viability (calculated with respect to control cells treated with DMSO alone) of three different experiments (n = 3).

5 DISCUSSION

Malignant Pleura Mesothelioma (MPM) is a highly aggressive malignancy for which there are no curative treatments [25]. Two major factors contribute to the poor prognosis of MPM: the disease is frequently detected at advanced stage, and it is very resistant to current standard therapy regimens [77]. Thus, there is an urgent need for the development of innovative therapeutic strategies.

MPM is characterized at the molecular level by the dysregulation of tumour suppressor genes [78], which are more difficult to "target" and reactivate than oncogenes, whose function should be inhibited [79]. The mutation/loss of the *INK4A/ARF* gene locus, the deletion of *NF2, the gene* encoding the Merlin protein, and changes in *BAP1* gene, are the most frequent genetic alterations found in this tumour [80]. Specifically, the alteration of the *INK4A/ARF* gene locus is responsible for the deletion, via alternative splicing mechanisms, of two important cell cycle regulators: the inhibitors p14 and p16, which are both involved in the regulation of the two most important cell cycle regulators, p53 and pRB1/p105, respectively. This protein is a member of the family of retinoblastoma proteins, which also includes pRBL1/p107 and pRBL2/p130 [81].

Proteins of the retinoblastoma family play a crucial function in modulating cell cycle progression [82]. Cyclin-dependent kinases (CDKs) complexes phosphorylate RBs to inhibit the RB–E2F interaction. RB proteins directly and indirectly suppress CDK activity and interact with chromatin-regulating and histone-modifying enzymes to drastically impact global gene expression and regulate both transitory and permanent cell-cycle exit RBL2/p130 dysregulation is a diagnostic and prognostic marker for several tumor types [82]. Due to RB protein and pathway dysregulation in cancer, various attempts are underway to move RB-based therapeutic treatments to the clinic

[82].Strategies that specifically target RB deficient cells have been designed, as well as strategies aimed at restoring RB canonical cell-cycle restraining function through CDK inhibition. RB proteins promote cell-cycle arrest or apoptosis. Thus, RB status is essential for predicting patient response to cytostatic or cytotoxic therapy. RB proteins can either prevent or cause apoptosis [82]. RBL2/p130 induces apoptosis in osteosarcoma, retinoblastoma, and hamster glioblastoma. Recently, we showed that inhibiting CDK2-mediated inhibitory phosphorylation of RBL2/p130 caused apoptosis in numerous cancer cell lines, including mesothelioma [82].

However, the mechanisms of pRB2 action remain to be fully defined. Our research group had recently demonstrated that reactivation of the pRBL2/p130 tumor suppressor mediates apoptosis in MPM cells, by counteracting the antiapoptotic pathway activated by AKT [59]. We identified RBL2/p130 as a new direct target of the AKT kinase and demonstrated that, in addition to its function of inhibiting the cell cycle, RBL2/p130 plays an active proapoptotic role in a variety of cancer cell types. Due to the fact that RBL2/p130 is altered in cancer, strategies aiming at activating its tumor suppressor potential could be an effective method for treating various malignancies. For example, using drugs that block cyclin-CDK complexes that caused the phosphorylation and inactivation of pocket proteins. So, we decided to test the cyclin-dependent kinase (CDK) 4/6 inhibitors a novel family of drugs that inhibit cell cycle progression to stop the growth of malignant cells.

We initially tested three of the new generation CDK 4/6 inhibitors: palbocilib, ribociclib and abemaciclib on a panel of MPM cell lines. The pharmacokinetics and pharmacodynamics of these three drugs share several similarities. However, due to some differences, the choice of a specific CDK4/6 inhibitor for a certain patient can be important. Palbociclib, ribociclib, and abemaciclib display modest differences in kinase selectivity [83]**.**Palbociclib and ribociclib were associated

with significant rates of hematological toxicity, including neutropenia, and low rates of serious infections. In most cases, abemaciclib caused high incidence of grade 1–2 gastrointestinal toxicities, especially diarrhea. Ribociclib was linked to a significant incidence of hepatotoxicity, respiratory toxicity, and QTc prolongation [83].

CDK4 is an important oncogenic driver of breast cancer, while CDK6 plays a crucial role in differentiation of hematopoietic stem cells Abemacliclib is approximately five times more potent against CDK4 than CDK6, suggesting that it could cause less hematological damage. In preclinical trials, palbociclib inhibited CDK4 and CDK6 with half maximum inhibitory doses (IC50) of 9–11 nM and 15 nM (ratio IC50 CDK4:CDK6 is 1:1.5), ribociclib with 10 nM and 39 nM (1:4), and abemaciclib with 2 nM and 9.7 nM (1:5). In contrast, abemaciclib inhibited CDK9 as well. These three inhibitors, palbociclib, ribociclib, and abemaciclib, are approved for breast cancer treatment in a wide range of settings and combination regimens [83].

Our data showed that abemacilib was effective in inhibiting cell proliferation of MPM cells at very low doses without major toxicity for normal mesothelial cells, in agreement with previously published data in breast cancer. Notably, abemaciclib was also effective in inhibiting the growth of MPM lines, derived from the most aggressive sarcomatoid histotype, which is often unresponsive to chemotherapeutic treatments [84]. This effect was evaluated both in the short term, using the MTS assay, and in the long term, using the clonogenic assay. In term of mechanisms our data indicated that the drug induced apoptosis in all MPM cell lines.

We also evaluated the impact of the inhibitor on the pocket proteins' activity. Abeamciclib significantly lowered the levels of Ser 975, Ser 941 and Ser 780 phosphorylation on RBL1/p107, RBL2/p130 and RBL1/p105 respectively. This is significant as in fact, these phosphorylation

events inhibit their tumor suppressor action. These results are consistent with what reported in the literature. In fact, abemaciclib should directly inhibit the cyclin-CDK4/6 complexes responsible for this phosphorylation, which regulates the interaction with E2F family transcriptional factors [85] [59] [86].

The effect of abemaciclib in restoring RB activity in MPM cells was associated with a downregulation of AKT activity, which affected MPM cell growth.

Conventional *in vitro* drug screening platforms utilize two-dimensional (2D) cell culture models that not fully recapitulate the *in vivo* three-dimensional (3D) tissue environment, and this might generate different drug responses. Recent advances in tissue engineering have produced the development of 3D cell culture techniques, which more properly recreate cell–cell and cell–extracellular matrix interactions as well as replicate the intricate microarchitectures observed in real tissues. Thus, cells grown as spheroids are a more accurate representation of *in vivo* cell growth [87]. Spheroids exhibit heterogeneity comparable to that of *in vivo* tumours. In the periphery of a spheroid, cells are proliferating, whereas cells deep in the spheroid are non-cycling. In addition, the center of the aggregate is usually formed by a necrotic and hypoxic core [88] (**Fig.23**). Multicellular resistance acquired by tumour cells can limit the success of therapeutic approaches. However, *in vitro* multicellular cancer spheroids are useful preclinical models for drug resistance, bridging the complexity gap between monolayer culture and tumour microenvironment [89].

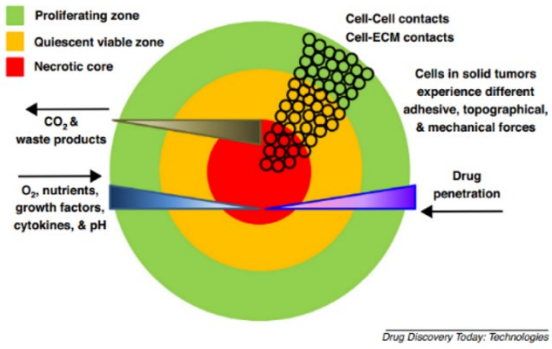

Representation of a multicellular spheroid (Sant and Johnston)

Figure 23

Hamamoto et al. demonstrated that CDK inhibitors, p21 and p27, were highly expressed in spheroids [90]. Moreover, they demonstrated that CDK4 overexpression increased spheroid

formation of glioma cells, while CDK4 knockdown significantly inhibited this process [91]. Thus, based on the data showing the role of CDK4 in regulating spheroid formation, we demonstrated that targeting CDK 4/6 with abemaciclib inhibited the formation of first generation MPM spheroids, which are spheroids formed from cells previously seeded in monolayer culture. To be most effective, anticancer drugs must efficiently infiltrate tissue and reach sufficient concentrations of cancer cells within the target population to provide a therapeutic efficacy. Most of the research into chemotherapy resistance of cancer has focused on the molecular mechanisms of resistance, but the impact of limited drug distribution within tumours has been widely ignored [92]. Our data show that abemaciclib reached the target population and inhibit growth of two-days old MPM spheroids and we also demonstrated that abemaciclib penetrated deep into the spheroids and inhibited proliferation of second-generation spheroids (spheroids that developed from first-generation spheroids). We have also demonstrated that the RB proteins do not have any important role in MPM spheroids formation after testing spheroid shape, number, and dimension in MPM cells where we depleted pocket proteins.

The most advanced systemic treatment for unresectable and advanced MPM is chemotherapy consisting in a combination of cis- or carboplatin and pemetrexed, an antifolate [93].Similar to most other solid tumors, MPM may recur due to acquired chemotherapy drug resistance. Resistance to chemotherapeutic drugs is a significant obstacle to the efficacy of chemotherapy. Since just a few active agents are available for MPM care, resistance to these drugs suggests failure of chemotherapy [94]. Resistance to cisplatin and other chemo drugs are directly related to the stage of tumor progression as in fact cancer cells acquire additional genetic and epigenetic alterations that confer growth advantages and consequently, the expected cytotoxic or cytostatic effect does not occur [76]. We developed mesothelioma cells resistant to cisplatin treatment. These

cells were then exposed to abemaciclib, and we assessed the sensitivity to this drug. After 72 hours of treatment the biphasic histotype cells showed a significative resistance to abemaciclib at low concentration but not to higher. In contrast, the most aggressive histotype was sensitive to abemaciclib at any concentrations. This suggest that abemaciclib could be an effective chemotherapy to MPM patients who have develop resistance to cisplatin.

In conclusion, the data obtained suggest that the inhibition of cyclin-CDK complexes and consequent reactivation of pocket proteins may represent a new potential therapeutic strategy for MPM. The data support that the phosphorylation status of retinoblastoma family proteins could serve as a biomarker to monitor endpoints for potential clinical trials using CDKs inhibitors. In addition, this work showed the effectiveness of abemaciclib on MPM cells and to MPM cell resistant to cisplatin. The results of these experiments are very promising and justify further studies which might help in improving MPM therapy.

Bibliography

[1] S. E. Mutsaers, 'The mesothelial cell', *Int J Biochem Cell Biol*, vol. 36, no. 1, pp. 9–16, Jan. 2004, doi: 10.1016/s1357-2725(03)00242-5.

[2] D. Whitaker, J. M. Papadimitriou, and M. N. Walters, 'The mesothelium and its reactions: a review', *Crit Rev Toxicol*, vol. 10, no. 2, pp. 81–144, Apr. 1982, doi: 10.3109/10408448209041321.

[3] M. A. Jantz and V. B. Antony, 'Pathophysiology of the pleura', *Respiration*, vol. 75, no. 2, pp. 121–133, 2008, doi: 10.1159/000113629.

[4] 'Malignant peritoneal mesothelioma: a review - PubMed'. https://pubmed.ncbi.nlm.nih.gov/30450291/ (accessed Jan. 20, 2023).

[5] I. Tischoff and A. Tannapfel, '[Mesothelioma]', *Pathologe*, vol. 38, no. 6, pp. 547–560, Nov. 2017, doi: 10.1007/s00292-017-0364-z.

[6] Alessandro Marinaccio Francesco Carrozza e gruppo di lavoro ReNaM, Alessandra Binazzi, Michela Bonafede1, Claudia Branchi, and Marcella Bugani, 'Sesto Rapporto Renam. Collana Ricerche'. 2018.

[7] F. Galateau-Salle, A. Churg, V. Roggli, W. D. Travis, and World Health Organization Committee for Tumors of the Pleura, 'The 2015 World Health Organization Classification of Tumors of the Pleura: Advances since the 2004 Classification', *J Thorac Oncol*, vol. 11, no. 2, pp. 142–154, Feb. 2016, doi: 10.1016/j.jtho.2015.11.005.

[8] M. B. Beasley, F. Galateau-Salle, and S. Dacic, 'Pleural mesothelioma classification update', *Virchows Arch*, vol. 478, no. 1, pp. 59–72, Jan. 2021, doi: 10.1007/s00428-021-03031-7.

[9] G. L. Ceresoli *et al.*, 'Therapeutic outcome according to histologic subtype in 121 patients with malignant pleural mesothelioma', *Lung Cancer*, vol. 34, no. 2, pp. 279–287, Nov. 2001, doi: 10.1016/s0169-5002(01)00257-4.

[10] I. Tischoff, M. Neid, V. Neumann, and A. Tannapfel, 'Pathohistological diagnosis and differential diagnosis', *Recent Results Cancer Res*, vol. 189, pp. 57–78, 2011, doi: 10.1007/978-3-642-10862-4_5.

[11] W. T. Vigneswaran *et al.*, 'Amount of Epithelioid Differentiation Is a Predictor of Survival in Malignant Pleural Mesothelioma', *Ann Thorac Surg*, vol. 103, no. 3, pp. 962–966, Mar. 2017, doi: 10.1016/j.athoracsur.2016.08.063.

[12] A. Fassina *et al.*, 'Epithelial-mesenchymal transition in malignant mesothelioma', *Mod Pathol*, vol. 25, no. 1, pp. 86–99, Jan. 2012, doi: 10.1038/modpathol.2011.144.

[13] P. Beckett, J. Edwards, D. Fennell, R. Hubbard, I. Woolhouse, and M. D. Peake, 'Demographics, management and survival of patients with malignant pleural mesothelioma in the National Lung Cancer Audit in England and Wales', *Lung Cancer*, vol. 88, no. 3, pp. 344–348, Jun. 2015, doi: 10.1016/j.lungcan.2015.03.005.

[14] J. Obacz *et al.*, 'Biological basis for novel mesothelioma therapies', *Br J Cancer*, vol. 125, no. 8, pp. 1039–1055, Oct. 2021, doi: 10.1038/s41416-021-01462-2.

[15] A. C. Bibby *et al.*, 'Malignant pleural mesothelioma: an update on investigation, diagnosis and treatment', *Eur Respir Rev*, vol. 25, no. 142, pp. 472–486, Dec. 2016, doi: 10.1183/16000617.0063-2016.

[16] L. A. Cox, 'Dose-response modeling of NLRP3 inflammasome-mediated diseases: asbestos, lung cancer, and malignant mesothelioma as examples', *Crit Rev Toxicol*, vol. 49, no. 7, pp. 614–635, Aug. 2019, doi: 10.1080/10408444.2019.1692779.
[17] E.-S. Lee and Y.-K. Kim, 'Asbestos Exposure Level and the Carcinogenic Risk Due to Corrugated Asbestos-Cement Slate Roofs in Korea', *Int J Environ Res Public Health*, vol. 18, no. 13, p. 6925, Jun. 2021, doi: 10.3390/ijerph18136925.
[18] A. Marinaccio, A. Binazzi, M. Bonafede, D. Di Marzio, A. Scarselli, and Regional Operating Centres, 'Epidemiology of malignant mesothelioma in Italy: surveillance systems, territorial clusters and occupations involved', *J Thorac Dis*, vol. 10, no. Suppl 2, pp. S221–S227, Jan. 2018, doi: 10.21037/jtd.2017.12.146.
[19] F. Baumann, J.-P. Ambrosi, and M. Carbone, 'Asbestos is not just asbestos: an unrecognised health hazard', *Lancet Oncol*, vol. 14, no. 7, pp. 576–578, Jun. 2013, doi: 10.1016/S1470-2045(13)70257-2.
[20] F. Baumann and M. Carbone, 'Environmental risk of mesothelioma in the United States: An emerging concern-epidemiological issues', *J Toxicol Environ Health B Crit Rev*, vol. 19, no. 5–6, pp. 231–249, 2016, doi: 10.1080/10937404.2016.1195322.
[21] C. Magnani *et al.*, 'III Italian Consensus Conference on Malignant Mesothelioma of the Pleura. Epidemiology, Public Health and Occupational Medicine related issues', *Med Lav*, vol. 106, no. 5, pp. 325–332, Sep. 2015.
[22] D. A. Altomare *et al.*, 'Activated TNF-alpha/NF-kappaB signaling via down-regulation of Fas-associated factor 1 in asbestos-induced mesotheliomas from Arf knockout mice', *Proc Natl Acad Sci U S A*, vol. 106, no. 9, pp. 3420–3425, Mar. 2009, doi: 10.1073/pnas.0808816106.
[23] H. Yang *et al.*, 'TNF-alpha inhibits asbestos-induced cytotoxicity via a NF-kappaB-dependent pathway, a possible mechanism for asbestos-induced oncogenesis', *Proc Natl Acad Sci U S A*, vol. 103, no. 27, pp. 10397–10402, Jul. 2006, doi: 10.1073/pnas.0604008103.
[24] K. Sinn, B. Mosleh, and M. A. Hoda, 'Malignant pleural mesothelioma: recent developments', *Curr Opin Oncol*, vol. 33, no. 1, pp. 80–86, Jan. 2021, doi: 10.1097/CCO.0000000000000697.
[25] P. Baas *et al.*, 'Malignant pleural mesothelioma: ESMO Clinical Practice Guidelines for diagnosis, treatment and follow-up', *Ann Oncol*, vol. 26 Suppl 5, pp. v31-39, Sep. 2015, doi: 10.1093/annonc/mdv199.
[26] Alessandro Marinaccio, Alessandra Binazzi, Claudia Branchi, and Marisa Corfiati, 'Registro Nazionale dei Mesoteliomi. Terzo Rapporto. Roma: Istituto Superiore per la Prevenzione e la Sicurezza del Lavoro'. 2010.
[27] A. Scherpereel *et al.*, 'ERS/ESTS/EACTS/ESTRO guidelines for the management of malignant pleural mesothelioma', *Eur Respir J*, vol. 55, no. 6, p. 1900953, Jun. 2020, doi: 10.1183/13993003.00953-2019.
[28] R. M. Rudd, 'Malignant mesothelioma', *Br Med Bull*, vol. 93, pp. 105–123, 2010, doi: 10.1093/bmb/ldp047.
[29] A. A. Renshaw, B. R. Dean, K. H. Antman, D. J. Sugarbaker, and E. S. Cibas, 'The role of cytologic evaluation of pleural fluid in the diagnosis of malignant mesothelioma', *Chest*, vol. 111, no. 1, pp. 106–109, Jan. 1997, doi: 10.1378/chest.111.1.106.

[30] J. L. Sauter *et al.*, 'The 2021 WHO Classification of Tumors of the Pleura: Advances Since the 2015 Classification', *J Thorac Oncol*, vol. 17, no. 5, pp. 608–622, May 2022, doi: 10.1016/j.jtho.2021.12.014.
[31] A. Jayaranagaiah *et al.*, 'Malignant Pleural Mesothelioma presenting with Cardiac Tamponade- A Rare Case report and Review of the literature', *Clin Case Rep Rev*, vol. 4, no. 5, 2018, doi: 10.15761/CCRR.1000414.
[32] 'Quaderni del ministero della salute N15. Diagnosi e terapia delle malattie asbesto-correlate non neoplastiche.' 2012.
[33] O. Abdel-Rahman, Z. Elsayed, H. Mohamed, and M. Eltobgy, 'Radical multimodality therapy for malignant pleural mesothelioma', *Cochrane Database Syst Rev*, vol. 1, no. 1, p. CD012605, Jan. 2018, doi: 10.1002/14651858.CD012605.pub2.
[34] A. G. Nicholson *et al.*, 'EURACAN/IASLC Proposals for Updating the Histologic Classification of Pleural Mesothelioma: Towards a More Multidisciplinary Approach', *J Thorac Oncol*, vol. 15, no. 1, pp. 29–49, Jan. 2020, doi: 10.1016/j.jtho.2019.08.2506.
[35] L. Berzenji and P. Van Schil, 'Multimodality treatment of malignant pleural mesothelioma', *F1000Res*, vol. 7, p. F1000 Faculty Rev-1681, 2018, doi: 10.12688/f1000research.15796.1.
[36] A. Santoro *et al.*, 'Pemetrexed plus cisplatin or pemetrexed plus carboplatin for chemonaïve patients with malignant pleural mesothelioma: results of the International Expanded Access Program', *J Thorac Oncol*, vol. 3, no. 7, pp. 756–763, Jul. 2008, doi: 10.1097/JTO.0b013e31817c73d6.
[37] G. Zalcman *et al.*, 'Bevacizumab for newly diagnosed pleural mesothelioma in the Mesothelioma Avastin Cisplatin Pemetrexed Study (MAPS): a randomised, controlled, open-label, phase 3 trial', *Lancet*, vol. 387, no. 10026, pp. 1405–1414, Apr. 2016, doi: 10.1016/S0140-6736(15)01238-6.
[38] A. D. Garg *et al.*, 'Pathogen response-like recruitment and activation of neutrophils by sterile immunogenic dying cells drives neutrophil-mediated residual cell killing', *Cell Death Differ*, vol. 24, no. 5, pp. 832–843, May 2017, doi: 10.1038/cdd.2017.15.
[39] 'A phase II trial of surgical resection and adjuvant high-dose hemithoracic radiation for malignant pleural mesothelioma - PubMed'. https://pubmed.ncbi.nlm.nih.gov/11581615/ (accessed Jan. 20, 2023).
[40] C. Cao, D. Tian, C. Manganas, P. Matthews, and T. D. Yan, 'Systematic review of trimodality therapy for patients with malignant pleural mesothelioma', *Ann Cardiothorac Surg*, vol. 1, no. 4, pp. 428–437, Nov. 2012, doi: 10.3978/j.issn.2225-319X.2012.11.07.
[41] A. Rimner *et al.*, 'Phase II Study of Hemithoracic Intensity-Modulated Pleural Radiation Therapy (IMPRINT) As Part of Lung-Sparing Multimodality Therapy in Patients With Malignant Pleural Mesothelioma', *J Clin Oncol*, vol. 34, no. 23, pp. 2761–2768, Aug. 2016, doi: 10.1200/JCO.2016.67.2675.
[42] K. Harrington, D. J. Freeman, B. Kelly, J. Harper, and J.-C. Soria, 'Optimizing oncolytic virotherapy in cancer treatment', *Nat Rev Drug Discov*, vol. 18, no. 9, pp. 689–706, Sep. 2019, doi: 10.1038/s41573-019-0029-0.
[43] V. W. Rusch *et al.*, 'Initial analysis of the international association for the study of lung cancer mesothelioma database', *J Thorac Oncol*, vol. 7, no. 11, pp. 1631–1639, Nov. 2012, doi: 10.1097/JTO.0b013e31826915f1.
[44] L. S. Goodman and M. M. Wintrobe, 'Nitrogen mustard therapy; use of methyl-bis (beta-chloroethyl) amine hydrochloride and tris (beta-chloroethyl) amine hydrochloride for

Hodgkin's disease, lymphosarcoma, leukemia and certain allied and miscellaneous disorders', *J Am Med Assoc*, vol. 132, pp. 126–132, Sep. 1946, doi: 10.1001/jama.1946.02870380008004.
[45] S. Farber and L. K. Diamond, 'Temporary remissions in acute leukemia in children produced by folic acid antagonist, 4-aminopteroyl-glutamic acid', *N Engl J Med*, vol. 238, no. 23, pp. 787–793, Jun. 1948, doi: 10.1056/NEJM194806032382301.
[46] N. Vasan, J. Baselga, and D. M. Hyman, 'A view on drug resistance in cancer', *Nature*, vol. 575, no. 7782, pp. 299–309, Nov. 2019, doi: 10.1038/s41586-019-1730-1.
[47] J. Crofton, 'Chemotherapy of pulmonary tuberculosis', *Br Med J*, vol. 1, no. 5138, pp. 1610–1614, Jun. 1959, doi: 10.1136/bmj.1.5138.1610.
[48] G. Bonadonna *et al.*, 'Combination chemotherapy as an adjuvant treatment in operable breast cancer', *N Engl J Med*, vol. 294, no. 8, pp. 405–410, Feb. 1976, doi: 10.1056/NEJM197602192940801.
[49] M. L. Citron *et al.*, 'Randomized trial of dose-dense versus conventionally scheduled and sequential versus concurrent combination chemotherapy as postoperative adjuvant treatment of node-positive primary breast cancer: first report of Intergroup Trial C9741/Cancer and Leukemia Group B Trial 9741', *J Clin Oncol*, vol. 21, no. 8, pp. 1431–1439, Apr. 2003, doi: 10.1200/JCO.2003.09.081.
[50] D.-W. Shen, L. M. Pouliot, M. D. Hall, and M. M. Gottesman, 'Cisplatin Resistance: A Cellular Self-Defense Mechanism Resulting from Multiple Epigenetic and Genetic Changes', *Pharmacol Rev*, vol. 64, no. 3, pp. 706–721, Jul. 2012, doi: 10.1124/pr.111.005637.
[51] T. Makovec, 'Cisplatin and Beyond: Molecular Mechanisms of Action and Drug Resistance Development in Cancer Chemotherapy', *Radiol Oncol*, vol. 53, no. 2, pp. 148–158, Mar. 2019, doi: 10.2478/raon-2019-0018.
[52] Amaldi F et al., *Biologia molecolare.* 2014.
[53] K. A. Schafer, 'The cell cycle: a review', *Vet Pathol*, vol. 35, no. 6, pp. 461–478, Nov. 1998, doi: 10.1177/030098589803500601.
[54] C. Giacinti and A. Giordano, 'RB and cell cycle progression', *Oncogene*, vol. 25, no. 38, pp. 5220–5227, Aug. 2006, doi: 10.1038/sj.onc.1209615.
[55] V. Caracciolo, K. Reiss, K. Khalili, G. De Falco, and A. Giordano, 'Role of the interaction between large T antigen and Rb family members in the oncogenicity of JC virus', *Oncogene*, vol. 25, no. 38, pp. 5294–5301, Aug. 2006, doi: 10.1038/sj.onc.1209681.
[56] D. Cobrinik, 'Pocket proteins and cell cycle control', *Oncogene*, vol. 24, no. 17, pp. 2796–2809, Apr. 2005, doi: 10.1038/sj.onc.1208619.
[57] B. E. Engel, W. D. Cress, and P. G. Santiago-Cardona, 'THE RETINOBLASTOMA PROTEIN: A MASTER TUMOR SUPPRESSOR ACTS AS A LINK BETWEEN CELL CYCLE AND CELL ADHESION', *Cell Health Cytoskelet*, vol. 7, pp. 1–10, 2015, doi: 10.2147/CHC.S28079.
[58] 'The retinoblastoma tumour suppressor in development and cancer - PubMed'. https://pubmed.ncbi.nlm.nih.gov/12459729/ (accessed Jan. 20, 2023).
[59] F. Pentimalli *et al.*, 'RBL2/p130 is a direct AKT target and is required to induce apoptosis upon AKT inhibition in lung cancer and mesothelioma cell lines', *Oncogene*, vol. 37, no. 27, pp. 3657–3671, Jul. 2018, doi: 10.1038/s41388-018-0214-3.

[60] S. Lim and P. Kaldis, 'Cdks, cyclins and CKIs: roles beyond cell cycle regulation', *Development*, vol. 140, no. 15, pp. 3079–3093, Aug. 2013, doi: 10.1242/dev.091744.
[61] R. Roskoski, 'Cyclin-dependent protein serine/threonine kinase inhibitors as anticancer drugs', *Pharmacol Res*, vol. 139, pp. 471–488, Jan. 2019, doi: 10.1016/j.phrs.2018.11.035.
[62] C. Sánchez-Martínez, L. M. Gelbert, M. J. Lallena, and A. de Dios, 'Cyclin dependent kinase (CDK) inhibitors as anticancer drugs', *Bioorg Med Chem Lett*, vol. 25, no. 17, pp. 3420–3435, Sep. 2015, doi: 10.1016/j.bmcl.2015.05.100.
[63] E. S. Knudsen *et al.*, 'CDK/cyclin dependencies define extreme cancer cell-cycle heterogeneity and collateral vulnerabilities', *Cell Rep*, vol. 38, no. 9, p. 110448, Mar. 2022, doi: 10.1016/j.celrep.2022.110448.
[64] M. Malumbres, 'Cyclin-dependent kinases', *Genome Biol*, vol. 15, no. 6, p. 122, 2014, doi: 10.1186/gb4184.
[65] W. Cheng *et al.*, 'Recent development of CDK inhibitors: An overview of CDK/inhibitor co-crystal structures', *Eur J Med Chem*, vol. 164, pp. 615–639, Feb. 2019, doi: 10.1016/j.ejmech.2019.01.003.
[66] E. S. Kim, 'Abemaciclib: First Global Approval', *Drugs*, vol. 77, no. 18, pp. 2063–2070, Dec. 2017, doi: 10.1007/s40265-017-0840-z.
[67] M. E. Klein, M. Kovatcheva, L. E. Davis, W. D. Tap, and A. Koff, 'CDK4/6 Inhibitors: The Mechanism of Action May Not Be as Simple as Once Thought', *Cancer Cell*, vol. 34, no. 1, pp. 9–20, Jul. 2018, doi: 10.1016/j.ccell.2018.03.023.
[68] S. La Monica *et al.*, 'Efficacy of the CDK4/6 Dual Inhibitor Abemaciclib in EGFR-Mutated NSCLC Cell Lines with Different Resistance Mechanisms to Osimertinib', *Cancers (Basel)*, vol. 13, no. 1, p. 6, Dec. 2020, doi: 10.3390/cancers13010006.
[69] 'In evidenza delle informazioni prescrittive per Verzenio'. 2017.
[70] 'Three-dimensional in vitro culture models in oncology research - PubMed'. https://pubmed.ncbi.nlm.nih.gov/36089610/ (accessed Jan. 20, 2023).
[71] M. Vinci *et al.*, 'Advances in establishment and analysis of three-dimensional tumor spheroid-based functional assays for target validation and drug evaluation', *BMC Biol*, vol. 10, p. 29, Mar. 2012, doi: 10.1186/1741-7007-10-29.
[72] L. Anders *et al.*, 'A systematic screen for CDK4/6 substrates links FOXM1 phosphorylation to senescence suppression in cancer cells', *Cancer Cell*, vol. 20, no. 5, pp. 620–634, Nov. 2011, doi: 10.1016/j.ccr.2011.10.001.
[73] B. R. Topacio *et al.*, 'Cyclin D-Cdk4,6 Drives Cell-Cycle Progression via the Retinoblastoma Protein's C-Terminal Helix', *Mol Cell*, vol. 74, no. 4, pp. 758-770.e4, May 2019, doi: 10.1016/j.molcel.2019.03.020.
[74] Y. Uchida *et al.*, 'Analogy between sphere forming ability and stemness of human hepatoma cells', *Oncol Rep*, vol. 24, no. 5, pp. 1147–1151, Nov. 2010, doi: 10.3892/or_00000966.
[75] B. Biersack, 'Relations between approved platinum drugs and non-coding RNAs in mesothelioma', *Noncoding RNA Res*, vol. 3, no. 4, pp. 161–173, Dec. 2018, doi: 10.1016/j.ncrna.2018.08.001.
[76] Y. Lugones, P. Loren, and L. A. Salazar, 'Cisplatin Resistance: Genetic and Epigenetic Factors Involved', *Biomolecules*, vol. 12, no. 10, p. 1365, Sep. 2022, doi: 10.3390/biom12101365.

[77] G. Bronte *et al.*, 'The resistance related to targeted therapy in malignant pleural mesothelioma: Why has not the target been hit yet?', *Crit Rev Oncol Hematol*, vol. 107, pp. 20–32, Nov. 2016, doi: 10.1016/j.critrevonc.2016.08.011.
[78] T. K. Hinz and L. E. Heasley, 'Translating mesothelioma molecular genomics and dependencies into precision oncology-based therapies', *Semin Cancer Biol*, vol. 61, pp. 11–22, Apr. 2020, doi: 10.1016/j.semcancer.2019.09.014.
[79] 'Mesothelioma treatment: Are we on target? A review - PubMed'. https://pubmed.ncbi.nlm.nih.gov/26257929/ (accessed Jan. 20, 2023).
[80] A.-M. Kukuyan *et al.*, 'Inactivation of Bap1 Cooperates with Losses of Nf2 and Cdkn2a to Drive the Development of Pleural Malignant Mesothelioma in Conditional Mouse Models', *Cancer Res*, vol. 79, no. 16, pp. 4113–4123, Aug. 2019, doi: 10.1158/0008-5472.CAN-18-4093.
[81] M. G. Paggi, A. Baldi, F. Bonetto, and A. Giordano, 'Retinoblastoma protein family in cell cycle and cancer: a review', *J Cell Biochem*, vol. 62, no. 3, pp. 418–430, Sep. 1996, doi: 10.1002/(SICI)1097-4644(199609)62:3%3C418::AID-JCB12%3E3.0.CO;2-E.
[82] P. Indovina, E. Marcelli, N. Casini, V. Rizzo, and A. Giordano, 'Emerging roles of RB family: new defense mechanisms against tumor progression', *J Cell Physiol*, vol. 228, no. 3, pp. 525–535, Mar. 2013, doi: 10.1002/jcp.24170.
[83] 'Inhibiting CDK4/6 in Breast Cancer with Palbociclib, Ribociclib, and Abemaciclib: Similarities and Differences - PubMed'. https://pubmed.ncbi.nlm.nih.gov/33369721/ (accessed Jan. 20, 2023).
[84] 'Pharmacological targeting of p53 through RITA is an effective antitumoral strategy for malignant pleural mesothelioma - PubMed'. https://pubmed.ncbi.nlm.nih.gov/24345738/ (accessed Jan. 20, 2023).
[85] M. Kitagawa *et al.*, 'The consensus motif for phosphorylation by cyclin D1-Cdk4 is different from that for phosphorylation by cyclin A/E-Cdk2', *EMBO J*, vol. 15, no. 24, pp. 7060–7069, Dec. 1996.
[86] X. Leng, M. Noble, P. D. Adams, J. Qin, and J. W. Harper, 'Reversal of growth suppression by p107 via direct phosphorylation by cyclin D1/cyclin-dependent kinase 4', *Mol Cell Biol*, vol. 22, no. 7, pp. 2242–2254, Apr. 2002, doi: 10.1128/MCB.22.7.2242-2254.2002.
[87] 'Vascularization Strategies in 3D Cell Culture Models: From Scaffold-Free Models to 3D Bioprinting - PubMed'. https://pubmed.ncbi.nlm.nih.gov/36498908/ (accessed Jan. 20, 2023).
[88] 'Cell culture as spheroids: an approach to multicellular resistance - Search Results - PubMed'. https://pubmed.ncbi.nlm.nih.gov/?term=Cell+culture+as+spheroids%3A+an+approach+to+multicellular+resistance (accessed Jan. 20, 2023).
[89] X. Xiang *et al.*, 'The development and characterization of a human mesothelioma in vitro 3D model to investigate immunotoxin therapy', *PLoS One*, vol. 6, no. 1, p. e14640, Jan. 2011, doi: 10.1371/journal.pone.0014640.
[90] 'Differentiation and proliferation of primary rat hepatocytes cultured as spheroids - PubMed'. https://pubmed.ncbi.nlm.nih.gov/9792921/ (accessed Jan. 20, 2023).
[91] 'CDK4/6 inhibition suppresses tumour growth and enhances the effect of temozolomide in glioma cells - PubMed'. https://pubmed.ncbi.nlm.nih.gov/32277580/ (accessed Jan. 20, 2023).

[92] ‘Drug penetration in solid tumours - PubMed’. https://pubmed.ncbi.nlm.nih.gov/16862189/ (accessed Jan. 20, 2023).
[93] C. C. L. M. Boons, M. W. VAN Tulder, J. A. Burgers, J. J. Beckeringh, C. Wagner, and J. G. Hugtenburg, ‘The value of pemetrexed for the treatment of malignant pleural mesothelioma: a comprehensive review’, *Anticancer Res*, vol. 33, no. 9, pp. 3553–3561, Sep. 2013.
[94] M. Kitazono-Saitoh *et al.*, ‘Interaction and cross-resistance of cisplatin and pemetrexed in malignant pleural mesothelioma cell lines’, *Oncol Rep*, vol. 28, no. 1, pp. 33–40, Jul. 2012, doi: 10.3892/or.2012.1799.